



**UNIVERSITA' POLITECNICA DELLE MARCHE**

**FACULTY OF ENGINEERING**

---

Master of Science in Biomedical Engineering Department of Industrial Engineering and  
Mathematical Sciences

**DEVELOPMENT OF A MEASUREMENT PROCEDURE FOR THE CHARACTERIZATION  
OF A SPECIAL MATTRESS FOR THE TREATMENT AND PREVENTION OF PRESSURE  
ULCERS.**

*Supervisor:*

**Prof. Lorenzo Scalise**

*Co-supervisor:*

**Ing. Luca Antognoli**

*Candidate:*

**Andrea Sandri**

*Academic Year* **2019 / 2020**



# INDEX

<b>1. INTRODUCTION</b> .....	1
1.1 PRESSION ULCERS.....	2
1.2 PRESSION ULCERS TREATMENT.....	6
<b>2. MATERIALS AND METHODS</b> .....	10
2.1 DCPRESSURE MATTRESS.....	10
2.1.1 HARDWARE.....	10
2.1.2 SOFTWARE.....	13
2.2 NOVEL PRESSURE CELL MATRIX.....	17
2.2.1 HARDWARE.....	17
2.2.2 SOFTWARE.....	18
2.3 MEASUREMENT SETUP.....	20
2.3.1 SINGLE CELL CHARACTERIZATION.....	20
2.3.1.1 SINGLE CELL STRESS TEST.....	20
2.3.1.2 SINGLE CELL EFFICACY TEST.....	21
2.3.2 MATTRESS CHARACTERIZATION.....	23
2.3.2.1 TEST PROTOCOL.....	23
2.3.2.2 SETUP.....	24
2.3.2.3 PROTCOL DESCRIPTION.....	25
2.3.2.4 PARTECIPANT SELECTION.....	28
2.3.2.5 LONG-TERM TEST.....	29
2.3.2.6 DATA DESCRIPTION.....	30
2.3.2.7 DATA PROCESSING.....	30
2.3.2.8 CALIBRATION CURVE.....	34
<b>3. RESULTS</b> .....	35
3.1 SINGLE CELL STRESS TEST.....	35

3.2 SINGLE CELL EFFICACY TEST.....	37
3.3 DCPRESSURE SUPINE AND LATERAL TEST.....	39
3.4 LONG-TERM TEST.....	57
3.5 CALIBRATION CURVE.....	58
<b>4. DISCUSSION.....</b>	<b>61</b>
<b>5. CONCLUSIONS.....</b>	<b>65</b>
<b>6. BIBLIOGRAPHY.....</b>	<b>66</b>

*I dedicate this work to my family, which always supported me during my studies and to my friends,  
who always believed in me. Thank you.*

## 1. Introduction

The aim of this thesis is to assess the efficiency and efficacy of a mattress for the treatment and prevention of a very common and spread complication to many diseases during hospitalization, that are Pressure Ulcers (PU).

PU, also known as pressure sores, bedsores, decubitus ulcers and pressure injuries, are wounds caused by a decreased local circulation due to a high interface pressure (IP) [1]. A prolonged weight of the body or a limb, mixed often to shear forces can cause pus, and remaining seated or lying for an extended period of time increases the risk of pressure ulcers development, because the tissue remains squashed between the underlying surface and the bone prominences [2-4]. A key study [5] evidenced that also a small amount of pressure for a couple of hours in normally sitting conditions could lead to pressure ulcer development, due to the weight redistribution over a smaller area [6-7], causing oxygen depletion in the underlying muscles and tissues [8].

Annually, PU affect an estimate of 250,000 to 500,000 individuals in Canada with an overall estimated prevalence of 26.0% in healthcare institutions. In Germany, the prevalence rate is estimated to be 10 to 25% among ward patients and as high as 30% in rehabilitation centers. In one Austrian public hospital, incidence rates were between 1.39% and 7.98% for Stage 1, 0.14% and 1.52% for Stage II, and 0% and 0.88% for Stage III PU [9].

These lesions can rapidly spread from an apparently surface lesion to a larger tissue breakdown, involving skin, muscle and bone. The impact of PU involves not only economic burdens for the healthcare providers, but also the individual suffering due to the impact on the patient's general physical health, body image, independence and level of control.

The benefits of prevention are clear; it is highly preferable to reduce the incidence of pressure sores rather than managing the deleterious impacts of this disease. In particular, for geriatric and stroke patients in acute/critical care settings, the PU are indeed a threat [10]. Among the victims due to this disease, the 73% are found in the group of the over 65 years old. In 2005, a research [11] found that 28.7% of intensive care units (ICU) are prone to develop a PU.

Many devices exist to slow down PU, especially in subjects with limited mobility or bedridden, and this condition coupled with a pathology that causes a weight increase is the worst condition

possible for the development of this pathology. Among the different devices the most common are the Alternating Pressure Air Mattresses (APAMs), which can be of two kinds: alternating pressure air replacements (APARs) and alternating pressure air overlays (APAOs) [12]. Even if studies comparing different APAMs proved that they are more efficient compared to the standard hospital mattresses, they also evidenced that two-cell ones are more efficient in relieving the contact interface pressure (CIP) rather than the three-cell ones, and no significant differences are found among the different two-cells APAMs.

The aim of this research is to study the effectiveness of a device composed by a large number of individual cells and in order to do so we will have to define a measurement procedure to assess its characteristics, with a high degree of reliability and repeatability.

## **1.1 Pressure Ulcers**

“A pressure ulcer is localized injury to the skin and/or underlying tissue usually over a bony prominence, as a result of pressure, or pressure in combination with shear” [1]. The CIP over a certain threshold causes the upset of blood, starving the area of oxygen and nutrients, and if this condition continues over a prolonged time it causes the tissue breakdown and leads to a pressure ulcer.

To help to understand the severity of damage to the skin from pressure, the National Pressure Injury Advisory Panel refined the definition of pressure injuries and during the NPIAP Staging Consensus Conference in 2016, Rosemont (Chicago, IL), introduced an updated version of the staging system for their classification (Fig. 1-6) [13]. The higher the stage, the more severe are the complications to the skin and the underlying tissues.

### *- Stage One (Fig. 1)*

A category/stage one pressure ulcer is superficial damage and the affected area of skin appears discolored (red in people white skin or purple/bluish in people with darker skin tones). The skin is not broken, but it may be painful, itchy and feel warm and squishy, or hard on touching.

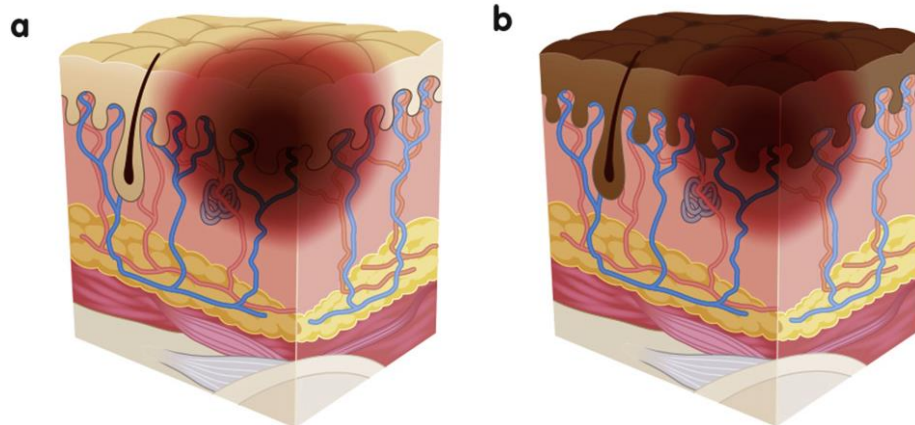


**Fig. 1** - a) Lightly pigmented: non blanchable erythema of intact skin. b) Darkly pigmented skin: erythema is not always visible.

- Stage Two (Fig. 2)

A category/stage two pressure ulcer presents a partial dermis thickness loss and appears as an open wound or a blister. It presents a shiny or dry shallow ulcer without slight or suspected deep tissue injury. This stage should not be used to describe skin tears, tape burns, perineal dermatitis, maceration or excoriations.

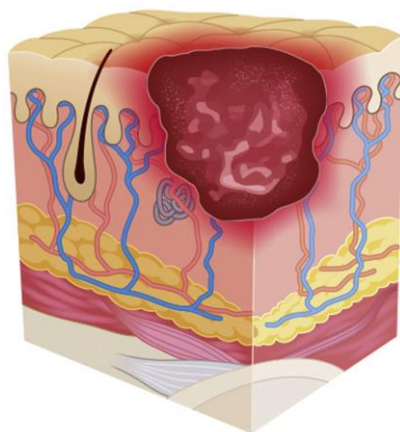


**Fig. 2** - Partial skin loss with exposed dermis.

- *Stage Three (Fig. 3)*

A category/stage three pressure ulcer can appear as a deep opening of the skin depending on the body location. The damage is both spread to skin and soft tissues and the subcutaneous fat may be visible, but bone, tendon or muscle are not exposed. Slough may be present but does not obscure the depth of tissue loss. It may include undermining and tunneling. Areas of significant adiposity can develop extremely deep stage-three PU.

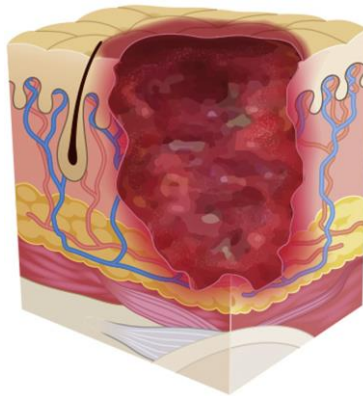


**Fig. 3** - Full thickness skin loss.

- *Stage Four (Fig. 4)*

A category/stage four pressure ulcer is the most severe type. Damage has occurred to the skin, soft tissue, and muscle; bone may often be visible, and the depth of the ulcer depends on the anatomical location. The bridge of the nose, ear, occiput and malleolus do not have subcutaneous tissue and these ulcers can be shallow. This kind of lesion can extend into muscle and/or supporting structures (i.e. fascia, tendon or joint capsule), making osteomyelitis possible. People who develop pressure ulcers of this category can develop life threatening infections and the bone/tendon is visible or directly palpable.

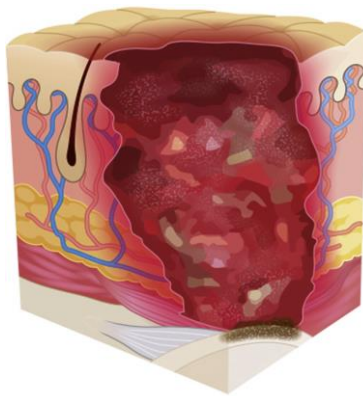


**Fig. 4** - Full thickness skin and tissue loss insert here.

- Stage Five (Fig. 5)

A stage five/unstageable pressure ulcer is covered with dead tissue and the extent of damage cannot be assessed until the dead tissue is removed by a trained healthcare professional. A suspected deep tissue injury is where the intact skin looks purple or brown in color or may have a blood-filled blister. This is due to damage of the soft tissue and on touching may be painful, firm, mushy, boggy, warm or cool.

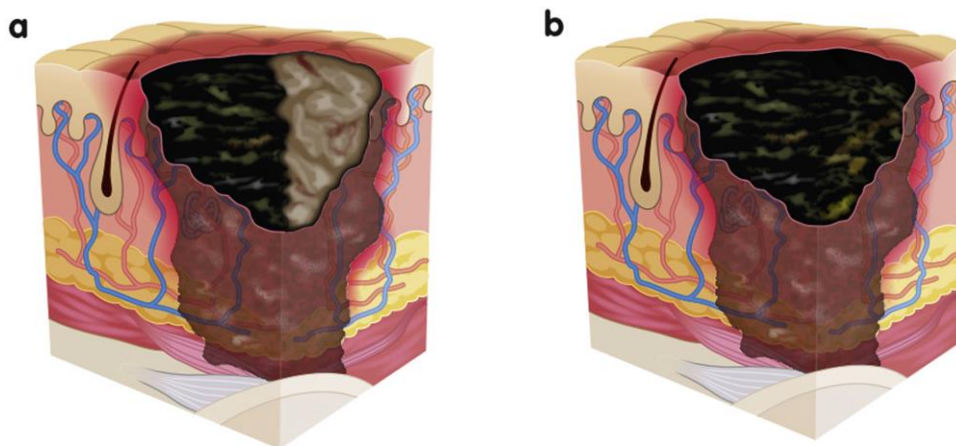


**Fig 5** - a) Slough and eschar insert here. b) Dark Eschar.

Under some circumstances the pressure over the skin can lead to a block of the capillary circulation, causing the death of the underlying tissues but without causing the external necrosis of the previous cases (Fig 6).

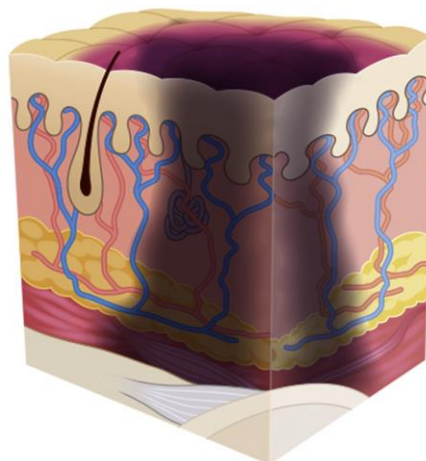


**Fig. 6** - Deep tissue pressure ulcer: persistent non blanchable deep red, maroon or purple discoloration. Suspected deep tissue injury.

The stages over the fifth severity stage can include many different complications due to the exposition of the underlying soft tissues, like a higher risk of infections or inflammation for the patient. This leads also to longer healing times and associated with higher incidence of complications and healthcare cost. For example, in the United States, the incidence of IV-stage pressure ulcers on the hospital treatment costs ranged from \$124,327 to \$129,248 USD, while in Canada the cost of PU management among individuals with a spinal cord injury in 2010 was \$4,475 CDN. In the UK, the estimated treatment cost associated with this disease varied from £1,214 to £14,108 per case [8].

## **1.2 Pressure ulcers treatment**

Despite various treatment methods for PU, the patient does suffer and often results in fatality due to decubitus ulcer. The major complications due to PU are the pain, discomfort and the patients become much more subject to secondary infections, like sepsis or osteomyelitis, causing an increasing in mortality [14]. The main treatment after the progression of the disease in the more advanced stages is the surgical reconstruction, which prolongs the hospital stay. The most common and widespread strategy for this kind of disease is prevention: there are two broad theories behind the etiology of its formation and are the neurogenic and mechanical one. In both cases the best way of intervention is prevention: in the first case the neurogenic intervention is to prevent the chance of occurrence of stroke and neurological pathologies, while in the second one is to prevent the excess of mechanical pressure under the ulcer vulnerable regions. The most common way to reduce the pressure on these locations is the use of devices to reduce the interface pressure or increasing the contact area, in order to decrease the overall pressure. This kind of devices can be divided into two kinds: static ones, that provide a constant redistribution of the force over an increasing skin contact surface and dynamic ones. This last kind makes the pressure vary cyclically, controlling the values of pressure of chambers inside the device to increase or decrease the interface contact area. Among the static devices we find mattresses, covers, cushions, wheelchair cushions and positioning support made from viscoelastic materials, memory foam gel, water or air. The dynamic devices include alternating low-air-mattresses, air fluidized beds, air cells with alternating insufflation or dynamic flotation systems [15].

The use of this kind of devices begins in 1975: a liner was designed with a restrainer which comprises of an extruded synthetic resin clip having a leg portion for retaining the clip in position relative to the interior surfaces of a water bed frame, a central portion bowed to provide a storage space and a spring bias and a head portion for bearing against the frame [16]. This bed suffered from the disadvantage that it could not elevate the patient whenever needed. Further improvements were made in subsequent design of a bed by which the patient could lie in an inclined position [17]. This bed resulted in more wear and tear beneath the trunk and gluteal regions because of shear and friction forces. Hence, later bed design had a flexible container for a waterbed of non-uniform depth, with maximum depth at an intermediate to provide an increased support [18]. Initially the interfacing surface was filled with hot water and the materials used as cushions were such as to maintain the temperature to prevent the chance of ulcer formation, using as heating source an external electrical source [19]. Further improvement used buoyant force to relieve the pressure [20], but maintenance of this waterbed was not simple. To make it easier, further bed designs provided for an airbed mattress and support system including an air reservoir and a device for controlled delivery of air to the airbed mattress. The user had the flexibility to control the air pressure in the airbed mattress [21]. In early 1990's this mattress came into market and were called 'alpha beds'. To provide more support and cushioning effect, foam containers were designed [22] and later it was improved with pulsating liquid foam container which would mimic an air circulating system [23].

Among the static and dynamic mattresses, many researches indicate the dynamic ones as more efficient [7, 9-12] in PU prevention and, in this work, we will characterize a particular kind of dynamic mattress. The aim of these devices is to bring the interface pressure level down to a continuously tolerable level, allowing the capillaries to continue perfusing the tissues, providing oxygen and nutrients and removing waste products and microthrombi. With an alternating pressure air mattress, the load on the skin is alternated and every area experiences pressure intermittently, allowing hypoxia and other metabolic deficits to be redressed in the interim. The different regions of the mattress are often pressurized at different levels, because the different body regions exert a different load on the contact area, due also to the different areas of the underlying bone prominences under these regions, like shown in *Fig. 7*.

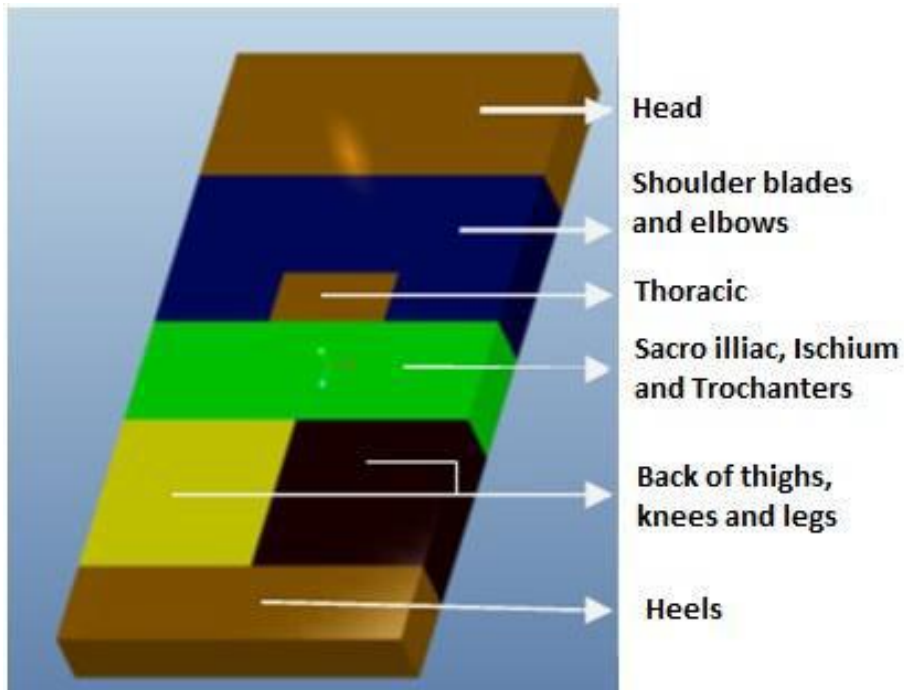


**Fig. 7** - Generally the active mattresses have different areas at different pressure levels.

The general functioning system of an active device is reported in *Fig. 8*.

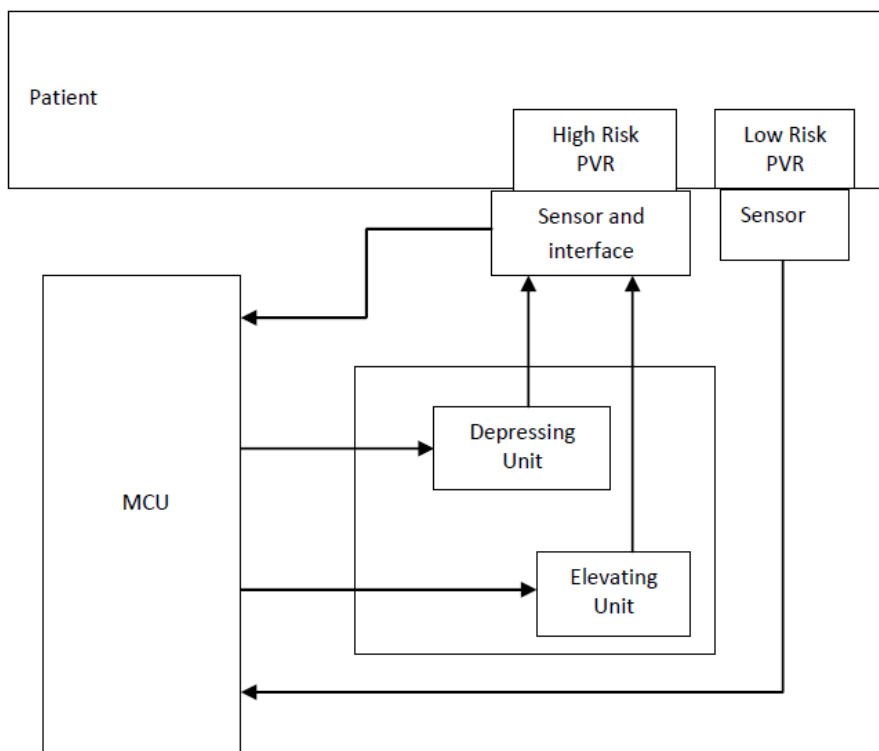


**Fig. 8** – General connection scheme of an APAM.

To measure the effectiveness of the device, we should look at the alert threshold that could compromise the local circulation in the contact areas. On this topic, this alert threshold level is different among many studies, but ranges between 20 and 40 mmHg [24] are often found in literature. This level is equal to the one of the capillaries of the tissues in contact with the surface. 30, 20, 10 mmHg are commonly used as pressure values respectively of capillaries, venules and veins pressure values (Fig. 9).

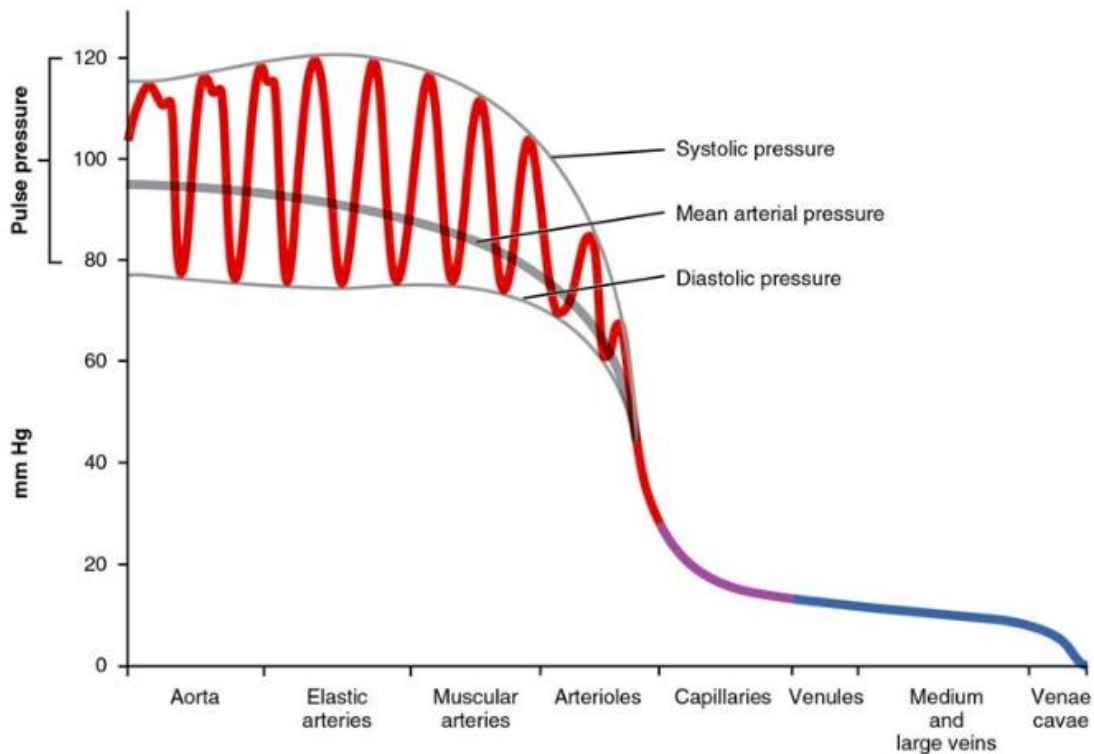


**Fig. 9** - Pressure values in the different body vessels. The capillary threshold value is commonly set to 30 mmHg.

Finding exactly the value relative to the threshold that could bring to the PU development is not easy, because in all the studies found in this research, many tied with different configurations, experimental setup and different aspects are commonly analyzed, like the ICP or blood oxygenation level. The non-existence of a standard widespread standard protocol makes very difficult to find a reference value. In addition, it is important to highlight that the risk of affecting the local circulation depends not only by the entity of the contact interface pressure, but also by the duration of application of this pressure on the affected area.

## 2. Materials and methods

In the following paragraphs the devices, procedures and obtained data will be explained. The hardware and software that is tested will be described, as well as the devices and instruments used in this characterization and the data processing.

### 2.1 The DCPressure mattress

In the following paragraph the DCPressure mattress hardware and software components will be described.

#### 2.1.1 DCPressure hardware

The mattress is composed by an array of 19 x 8 cells, for a total of 152 air chambers, connected each one in parallel through three-way valves to a bigger chamber surrounding the perimeter of the mattress (*Fig. 10*). The dimensions of a single cell is 10 x 10 x 12 cm.



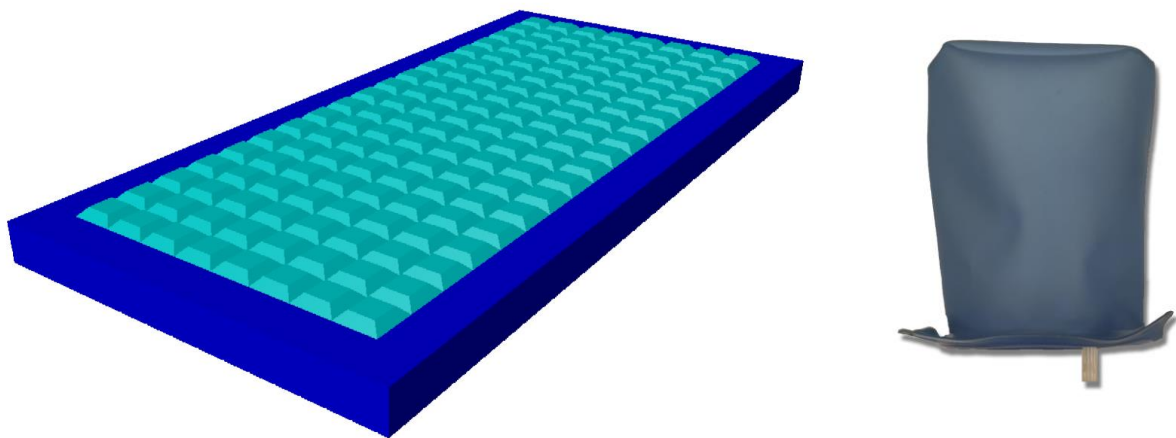
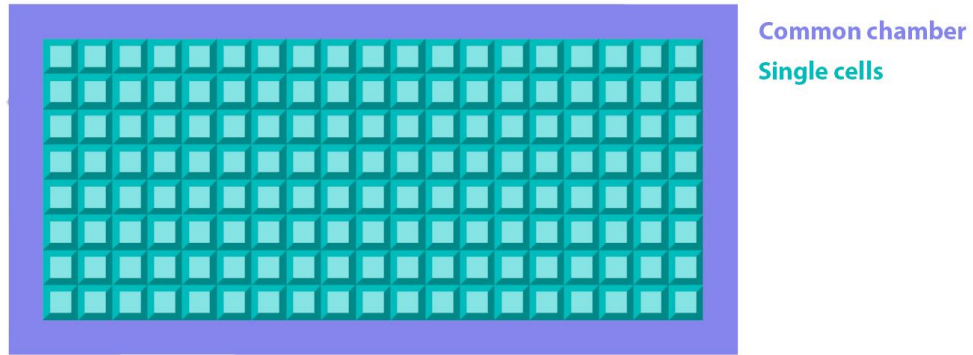


**Fig. 10** - The mattress is composed by an array of 19 x 8 cells (cyan), each one connected to a larger chamber (blue) surrounding the mattress. In the bottom right image, a single air chamber which composes the device.

The common chamber acts as air reservoir and is connected to a compressor; the opening and closing of the circuit is driven by a PC (Fig. 11), which controls the compressor behaviour and the opening of the three-way valve that puts in connection the chamber with the internal circuit, allowing the pressure to be inflated or deflated from the air reservoir to the single air chambers. The single cells valve opening, in series with the chamber valve allows a precise control on each single air chamber internal pression, according to the settings of the proprietary software.

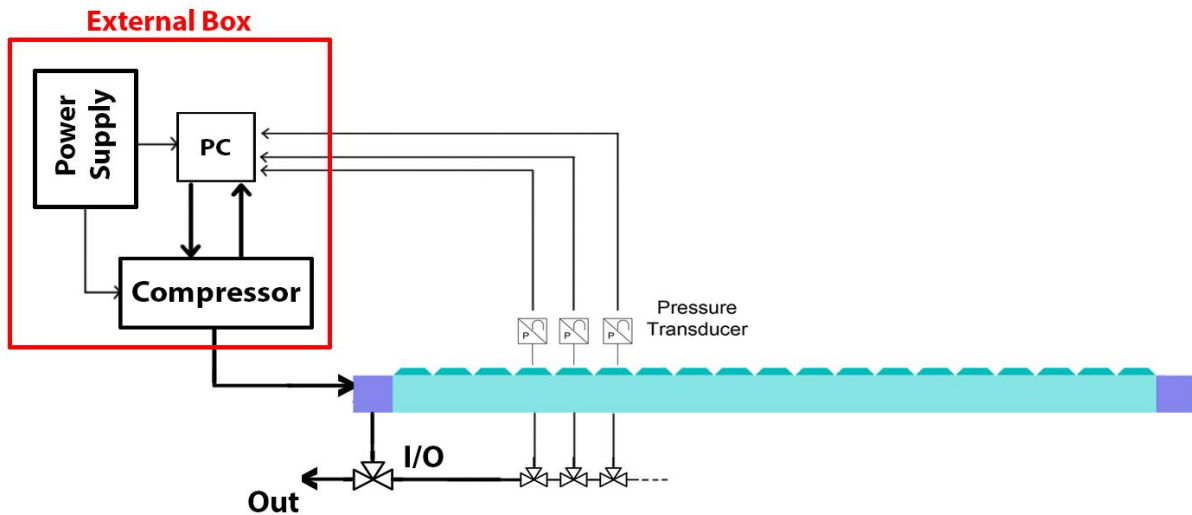


**Fig. 11** - Connection scheme between the mattress cells (cyan) and the larger chamber (blue), through three-way valves. All the cells are connected in parallel, each one with a controllable valve, to this larger chamber (blue), surrounding the mattress perimeter. This one is connected in series with the compressor through a three-way valve that allows the inflation or deflation of the circuit. The compressor is driven by a PC and this last can read the values of internal pressure of the single cells to perform regulations, thanks to pressure transducers in the air chambers.

All the components of power supply, PC, compressor and its valves are enclosed within a metal box of 39 x 47 x 16 cm, as seen in Fig. 12; the output and input can be given using a standard monitor, keyboard and mouse connected to the PC inside the box.



**Fig. 12** - Hardware components inside the case and their connenctions.

The system can be adjusted through preset routines that will be better described later in the chapter dedicated to the software, or the single cells can be manually regulated by the user. The compressor valves can be set to inflate or deflate, or the user may let the system to automatically adjust the internal pressure of the single cells in order to achieve a setpoint pressure. Also, the offset between the internal pressure and the one that must be achieved can be set by the user, but values too small will increase the number of regulation cycles needed and the initialization time. The cells composing the mattress can be divided into 4 groups, the first including the 1<sup>st</sup> rows 1-3, the second rows 4-12, the 3<sup>rd</sup> rows 13-17, the 4<sup>th</sup> rows 18-19. The different setpoints of the different groups are calculated as percentage increments or decrements of a single standard setpoint. During the tests the preset value of 70 daPA (0.70 kPa) has been maintained and all the standard pressures of the different groups have been maintained as standard: 0.77 kPa for the 1<sup>st</sup> group, 0.56 kPa for the 2<sup>nd</sup>, 0.49 kPa for the 3<sup>rd</sup> and 0.35 kPa for the 4<sup>th</sup> group.

### **2.1.2 DCPressure Software**

This device is able to work online and offline (locally). In the first case, if the system is online and connected to the host via a log interface, requiring an ID and password, and can be completely controlled remotely. In the second case, the system is controlled accessing the local PC and can be started manually without the need of an online connection. During this characterization, the system has been used always in this second mode. The mattress software interface is shown in *Fig. 13*, while the commands can be accessed right clicking on the icon in the bottom right of the Windows instruments bar and are shown in detail in *Fig. 15*. This interface presents the mattress cells divided by 19 rows and 8 columns. The green cell in the upper part, on the left, indicates the pressure level of the perimetral chamber of the mattress, connected to each single cell; all the values in this interface are expressed in Pa. P, T and R are indicators of the status of the valve that connects the air reservoir connected to the compressor to the internal circuit, indicating if it is inflating, deflating or in auto-regulation mode respectively. If the user manually sets the valve in P or T mode, the single cells pressure values can be adjusted, opening them with the P indicator in the lower left angle of the cells squares.

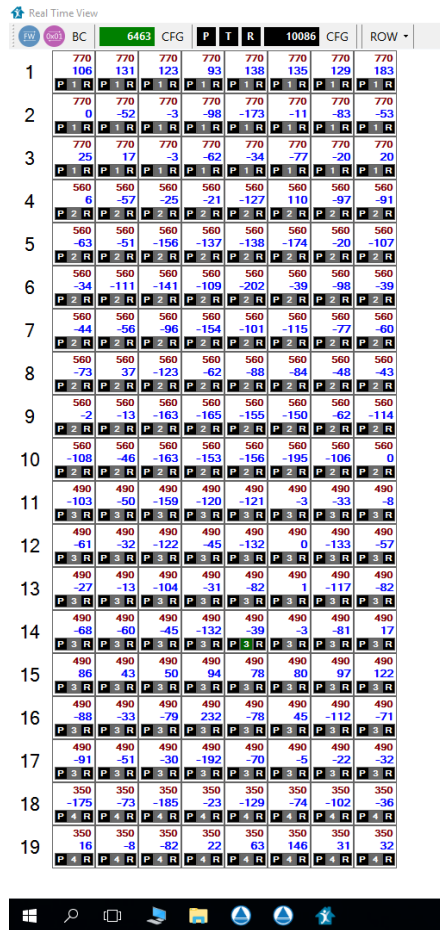


**Fig. 13** - Mattress main interface: we have the values, expressed in daPa, relative to the single cells of the 19x8 array. The values in red are relative to the setpoints, while the blue ones to the current pressure in the air chambers. On top, the pression inside the perimetral chamber, the compresor valves status and the atmospheric pressure.

The R button will let the system work autonomally, trying to set the cells inner pressure to the level expressed in red, which is the aim level for that cell, while the blue one is the one currently recorded by the system. The value in the black cell on the top is the current atmospheric pressure, which is needed by the software to perform the automatic adjustments, due to the fact that the valves are not differential. The “ROW” button opens a drop down menu which allows the user to select the rows that he wants to refresh during the reading scan, allowing to select all or none of them or to invert an existing selection. The selection can be performed also manually clicking on the row we are interested to scan. The cells reading is performed sequentially from the left to the right starting form the upper selected rows. If there are more rows selected, the refresh rate of the displayed values will be lower, but the single cells reading can be controlled frame by frame clicking on a cell, which will open a new window, shown in Fig. 14.

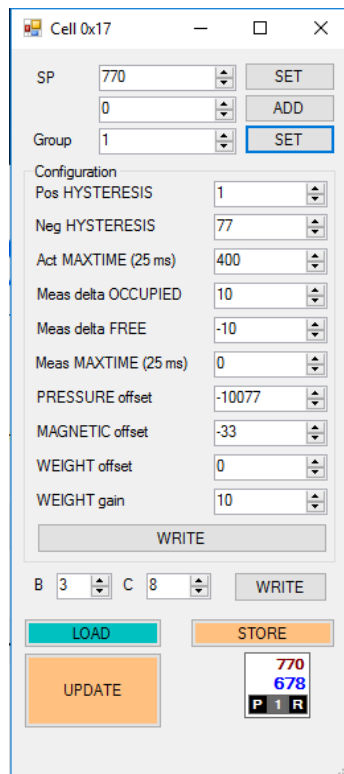


**Fig. 14** - Control window of a single cell.

The most important value to control in this window is the “SP” one, which is the setpoint that the cell will try to achieve in the Initialization mode. As we can see from the setpoint values (red) in *Fig. 13*, the mattress cells are divided into four groups, each region with a specific threshold value to achieve, due to the comfort optimization for the various body regions. The negative hysteresis, instead, is the maximal difference allowed between the actual pressure in the cells and the setpoint values during the Initialization mode. For all the tests regarding this characterization, the standard hysteresis values have been maintained, otherwise, if the maximal difference among the registered value and the SP is too small, the Initialization phase would last too long and the cells would be continuously automatically inflated and deflated.

The controls are accessible right-clicking in the bottom right icon in the instrument bar of the monitor and are shown in *Fig. 15*.

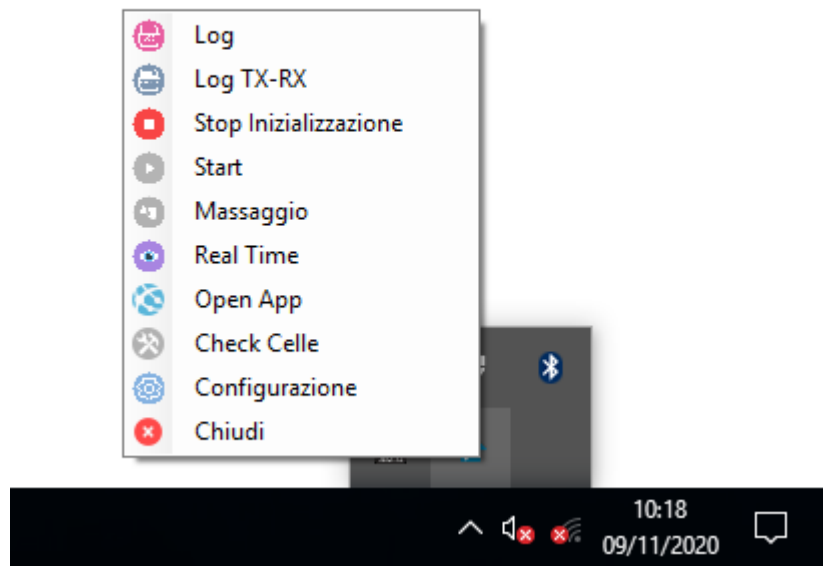


**Fig. 15** - The mattress controls are accessible right-clicking on the icon in the mattress software icon in the instrument bar.

The controls are, in order:

- *Log*: It will open the mattress database interface, accessible with an ID and password to control remotely the device.
- *Initialization/Stop Initialization*: It will start the mattress initialization phase; the system will try to make the single cells internal pression values equal to the relative setpoints.
- *Start*: The mattress, during the first 10 seconds, will inflate and deflate the cells in a checkboard manner, first the “whites” and then the “black”; confronting the pressure values of the cells, it is possible to understand which cells are active (i.e. there is something on them). After this initial process, the cells that are considered occupied are connected in a closed circuit, acting on their valves, and will try to homogenize the pression in these cells, and in this way also the ICP. It is important to underline that the data recording of the pression values of the single cells will be performed only in this mode.
- *Massage*: The cells will be inflated and deflated slightly in the checkboard manner described above, in order to avoid the complete immobility of the bedridden patient, and allowing an alternate pression relief on the interface skin.

- *Real Time*: It will open the window shown in *Fig. 13*, allowing the user to see the pressure values of the single cells and selecting the scan lines.

The other functions have not been used during this characterization. The output data are stored in a .dat file that contains the timestamp value corresponding to the time and date of acquisition, and the 152 values of pressure of the cells.

## 2.2 Novel® pressure cell matrix

The Novel® pressure cell matrix is composed by an array of 16x16 pressure sensors; each sensor covers an area of 6 cm<sup>2</sup>, for a total measuring area of 40x40cm.

### 2.2.1 Novel® hardware

The hardware is composed by the matrix, covering a total area of 40x40 cm of measurable area, shown in *Fig. 16*. The piezoelectric pressure sensors are characterized by a minimum measurable value of 1.25 kPa, a resolution of 0.25 kPa and a full-scale value of 63.75 kPa. The acquisition frequency can be controlled via software, and for this study the value of 1 Hz has been used.

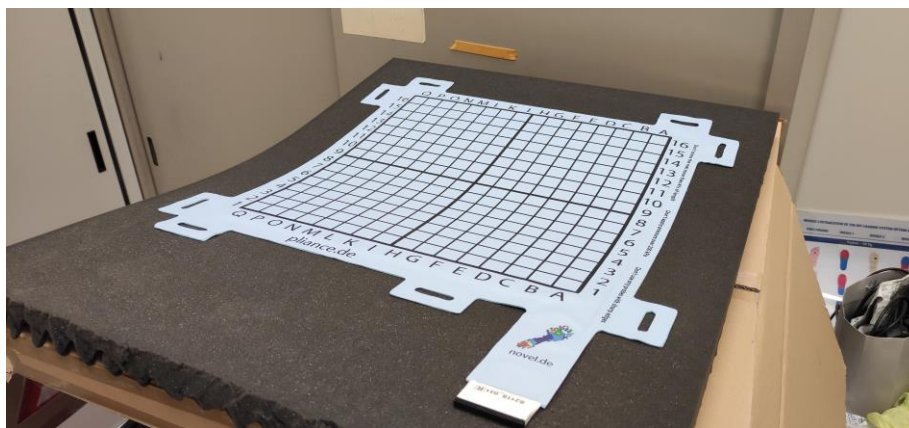


*Fig. 16* – Novel® pressure cell matrix.

The matrix is connected to a proprietary device that is able to be used with also other Novel® products and that is powered by a battery. This device is connected to a PC via bluetooth or fiber

optic cable (FOC): in our tests we used always this second connection method; the connection scheme is showed in *Fig. 17*.

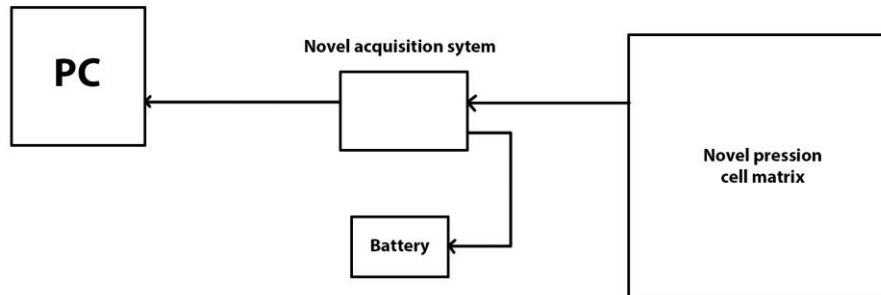


*Fig. 17* – Novel pression cell matrix connection scheme. The matrix is connected to a proprietary box, powered by a rechargeable battery. This box can be connected to the PC via bluetooth or FOC.

## 2.2.2 Novel® software

An example of the Novel® software user interface can be seen in *Fig. 18*. After a test connection between the components and a calibration using a provided configuration file, we can start the data acquisition. The acquisition frequency can be setted by the user; on the left panel we have a real time visualization of the pression values on the single sensors, while in the right panel we have the real time update of the graphs of peak pression [kPa], total force [N] on the matrix and active area [cm<sup>2</sup>]. This area can be also used to show the same data but in a bar visualization style, allowing to see the maximal value for each of the three measured output for each frame. Another aspect that the software allows is the creation of masks on the matrix, allowing to activate only single sensors or areas. Once the registration has been stopped, the software saves the file in a native .dat file in the novel folder, creating a subfolder with the acquisition date if the sujet name is not given, or creating a folder with the subject name if the user gave one. In this second phase, the user has the opportunity to move a cursor along the acquisition frames and see the values in that specific instant. The data can then be saved in .asc and .fgt, which will contain some specific information that will be better esposed later in the “Data description” chapter.

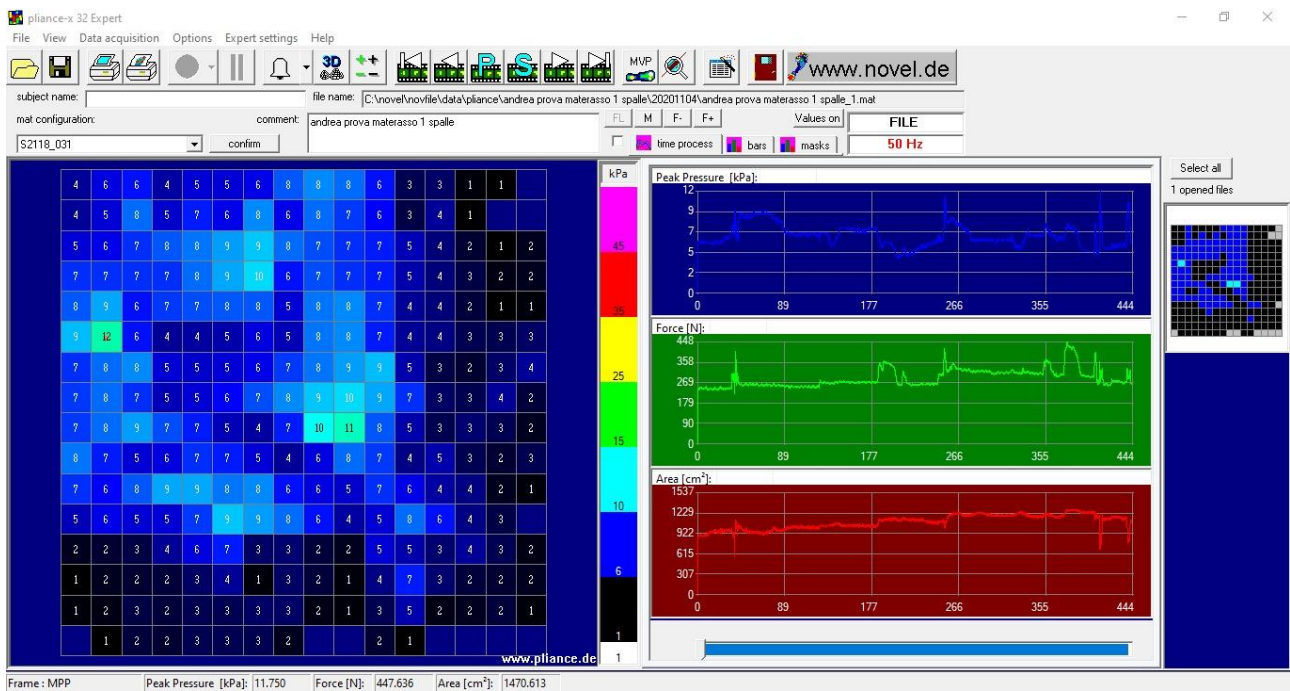


**Fig. 18** – Software user interface of the Novel® matrix. In this case we have an acquisition frequency of 50 Hz and we can see in the left the current pression values on the single sensors, while in the right we have the peak pressure [kPa], force [N] and total area [cm<sup>2</sup>].

The Novel® matrix allows to have as output a .asc and a .fgt file containing respectively the information about pressure of all the single cells for each sample, force integral [kPa], calculated as the area under the force curve, and maximum pressure time integral, calculated as the area under the maximal pressure curve. The second file contains information about the total force acting on the matrix at each recorded time instant, as well the components of COP displacement coordinates expressed in mm.

## **2.3 Measurement setup**

In the following section the performances of the single air chambers and the device in its overall functioning will be treated and the different performed tests will be explained.

### **2.3.1 DCPressure single cell characterization**

The aim of this test is to characterize not the DCPressure mattress in its total behaviour, but the characteristics of a single cell. These elements must withstand the weight of the bedridden patient for prolonged time, without undergoing deformations that would invalidate their operation or lead to mechanical failure. The single cells, during the Initialization phase, are inflated to a maximum SP value of 770 Pa (0.77 kPa).

#### **2.3.1.1 Single cell stress test**

A first test session was conducted to analyze the sealing limit of the air chamber and identify what type of critical issues it may show if subject to constantly increasing loads.

The test consists of a manually operated mechanical press that simulates a load above the air chamber: we start from an initial situation with the chamber inflated to a pressure slightly higher than the recommended operating pressure, in our case 100 mbar (10 kPa), and proceed by gradually increasing the load. Meanwhile, the values of internal pressure of the cell are showed by an analogic manometer and the load exercised is recorded by a load cell. A schematic representation of the test is reported in *Fig 19*. A total of two tests were carried out on two different chambers, both with an initial inflation of 100 mbar. The results can be found in the relative chapter.

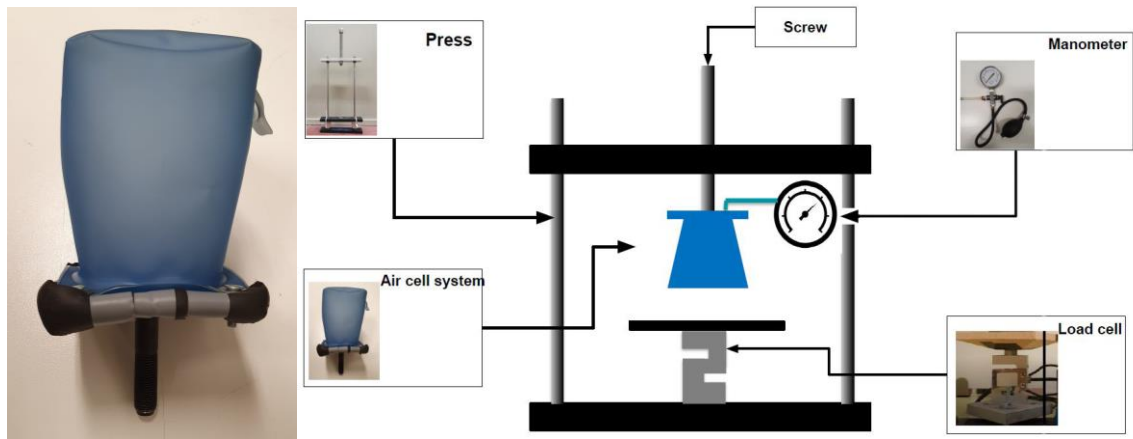


**Fig. 19** – In the left a single DCPressure mattress cell, while in the right the connection scheme of the components of this test.

A final test has been conducted exercising a higher load on the cell for a short period of time. The initial internal pressure of the cell is at 100 mbar; the test consists on exercising the load of the weight of a 70 Kg person on a single cell for a period of 1 second. In this test, the load cell couldn't be used, due to a sampling rate unsuitable for the test performed.

The tests carried out show that the air chamber resists up to a constant increasing load of a maximum of 700 N before being irreversibly deformed. The material that composes the chambers resists even higher loads for short period of time; in no case there was an explosive failure and no laceration of the cell was found.

### **2.3.1.2 Single cell efficacy test**

Once that the resistance of the single cell has been proved, we want to evaluate the effectiveness of the single cell in decreasing a localized peak pressure. To do so, we want to setup an experiment to measure the peak pressure produced by the Novel® pressure cell matrix in the initial condition, with an initial mattress cell internal pressure in the range of the initialization one, with a negative hysteresis allowed equal to the standard value, and comparing the same Novel® cells peak pressure after that only the correspondent mattress cell was manually deflated in a range between 0-100 Pa (0-0.1 kPa); the setup scheme is reported in Fig. 20.

The subject chosen for this test is a 50 Kg, 1,65 m high, 25 y.o. female. The area of interest is the shoulder; the subject has been placed laterally on the mattress, centering the area that will produce the highest Interface Contact Pressure (ICP), the greater tubercle, on a single mattress cell, the (6,5), as shown in red in *Fig. 21*. The green square in the figure represents the position of the Novel<sup>®</sup> matrix, placed in a way that the area corresponding to the interested mattress cell corresponds to a precise 4x4 Novel<sup>®</sup> cells subset.

The Novel<sup>®</sup> system has been placed between the mattress and the subject, with a light plastic sheet on it, to avoid a direct contact between some possible pointed areas of the clothes that could damage the sensors, with a sampling frequency of 1 Hz.

After a minute in which the subject is let settle in the chosen position, to avoid pressure peaks due to repositioning, we started the recording of the Novel<sup>®</sup> matrix sensors; in the mattress Real Time mode is not possible to record the cell pression data. In this way we can have a baseline to perform a comparison between the cell inflated at the setpoint and completely deflated. After a period of 48 seconds, the mattress cell corresponding to the greater tubercle is deflated, until reaching an internal pressure in the range 0-0.1 kPa. The total recording time has been of 190 seconds.

The maximal pression time evolution registered by the 4x4 Novel<sup>®</sup> cell array corresponding to the greater tubercle is reported in the “Results” paragraph.

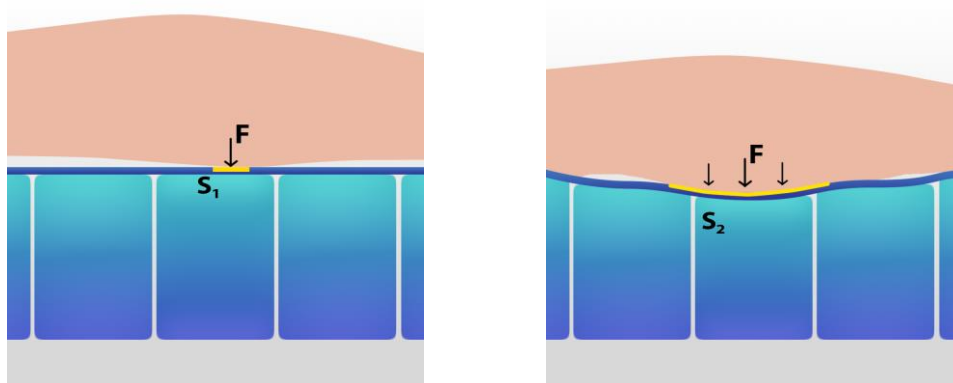


**Fig. 20** – The operative principle of the device consists in increasing the contact area in the points with the highest ICP, decreasing the localized pressure.

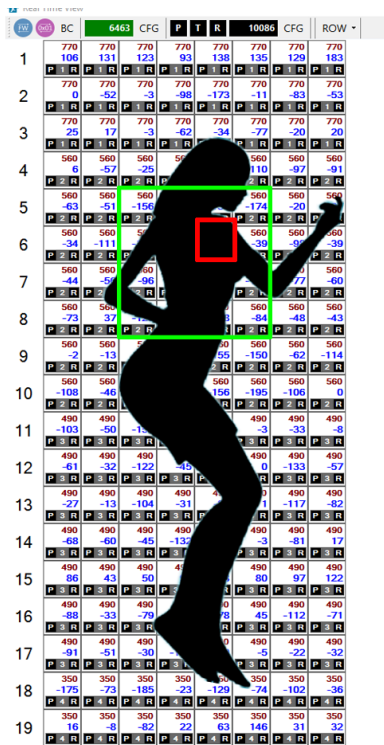


**Fig. 21** – Schematic representation of the placement of the subject on the mattress and relative positioning of the Novel® matrix (green) respect to the mattress. The interested cell that is deflated is the (6,5) mattress cell, corresponding to the greater tubercle (red).

## 2.3.2 Mattress characterization

This section will focus on assessing the performances of the mattress in its current setup, through the implementation of different test to assess the ability of decreasing the ICP, increasing the interface contact area and the ability of decreasing the areas where this value is over the threshold we are considering.

### 2.3.2.1 Test protocol

The aim of this section is to describe the tests performed to assess the effectiveness of the DCPressure mattress device, reconstructing a normal operating situation. The aim is to compare the measures given by the Novel® platform and the ones from the mattress ones in two different conditions, supine and lateral, and in four different areas for each condition. Unfortunately, the DCPressure records the values of internal pressure of the cells only in the Run mode, in which

before the mattress software starts understanding if there is someone on the mattress and then begins to join the interested cells to uniform and decrease the pressure.

### 2.3.2.2 Setup

The test consists in evaluating the effectiveness of the DCPressure mattress in decreasing the local interface contact pressure peaks in the most common areas subjected to this condition, which are the areas where the bone prominences are most exposed to form contact areas and exercise a pressure on the skin tissues. The areas most commonly subject to develop pressure sores are showed in *Fig. 22*, and are the back of the head, shoulders, elbows, buttocks and heels for the supine position, and ear, shoulder, elbow, hip, thigh and heel in the lateral position. Due also the fact that the positioning of bedridden patients in prone position is not common, if not in particular cases, during this study we considered only the conditions mentioned above.

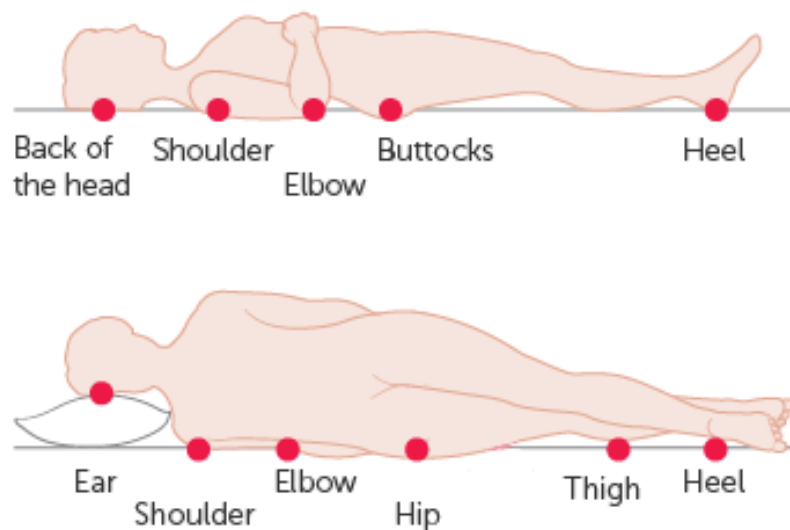


**Fig. 22** – Areas in supine (top) and lateral (bottom) lying position in which is more probable to develop PU.

The tests consists in evaluating the pression trend in these areas during the activation period of the device and measure the values recorded by the DCPressure cells and the Novel® matrix and compare them with the baseline values. A schematic representation of the setup is reported in *Fig. 23*.

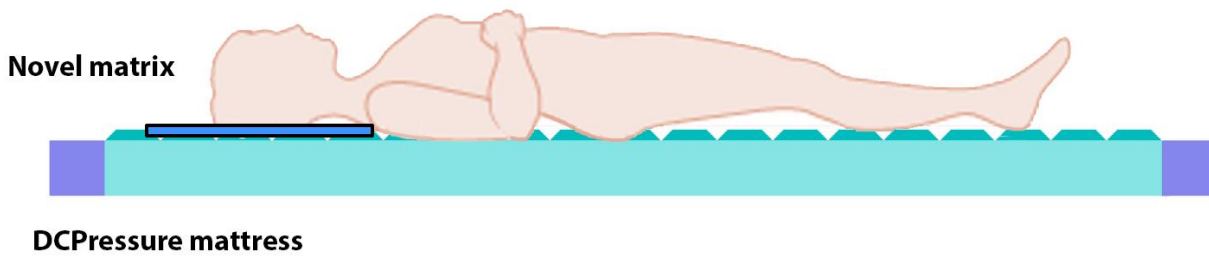


**Fig. 23** – Representation of the experiment setup. The subjects are positioned on the mattress and the Novel<sup>®</sup> matrix is put in between, to measure the interface contact pressure. The values of internal mattress cell pressure and ICP from the matrix are then used in the data processing phase.

### 2.3.2.3 Protocol Description

Due to the size of the Novel<sup>®</sup> matrix, that extends over an area of only 40x40 cm, we can cover the exact area of 16 mattress cells. For the supine position, we decided to consider the areas of the head, shoulders, hip and heels, while for the lateral position the shoulders/elbow, hip, the knee and heels. The Novel<sup>®</sup> pressure matrix has been placed always on the same mattress cells, because these ones have different initial setpoints for the internal pressure and to allow the inter-subject repeatability of the test and the possibility to compare the data.

In the lateral position, the head has not been considered as a dangerous zone because in a normal condition, when the patient is lying on a side is much more probable the use of a cushion.

The relative positioning of the Novel<sup>®</sup> matrix respect to the mattress cells are reported in *Fig. 24*; in all the conditions, the Novel<sup>®</sup> matrix was placed in the opposite direction of the mattress, because the Novel<sup>®</sup> software displays on the software the values in a way that the top left cell displayed is the bottom right on the matrix. Placing the matrix upwards allows a real time visualization of data on the Novel<sup>®</sup> software in the same direction in which the patient is lying.

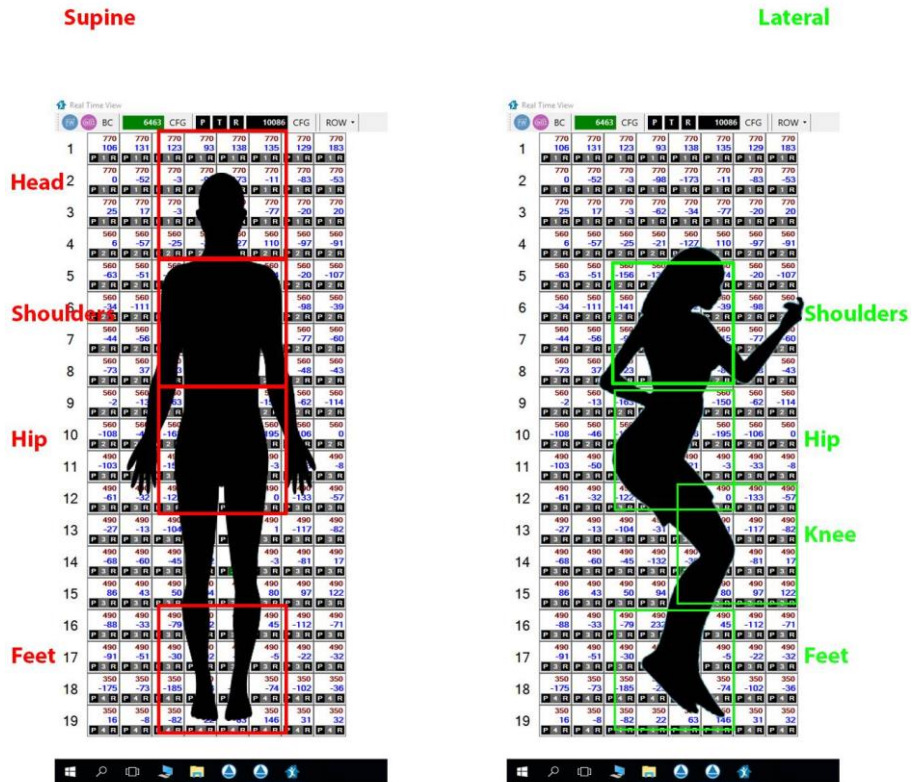


Fig. 24 – Relative displacement of the Novel® pressure sensor matrix in the supine and lateral lying conditions.

Being the Novel® platform always in the same positions, and having to be valid for different subjects, characterized by different heights and dimensions, a standard protocol has been established for each measured area:

Supine Position:

- *Head:* the subject is placed in a way that the rearmost part of the occipital lobe is centered in the center of the Novel® matrix, characterized by the cross of the two main thicker lines.
- *Shoulders:* the subject is placed in a way that the neck-shoulders line has is parallel to the second Novel® sensor row.
- *Hip:* the subject has been placed in such a way that the imaginary line connecting the great trochanters is parallel to the main horizontal central thicker line of the Novel® matrix.

- *Heels*: the subject has been placed in such a way that the imaginary line connecting the lateral malleoli is parallel to the main horizontal central thicker line of the Novel® matrix.

*Lateral Position:*

- *Shoulder*: the subject was placed in a way that the greater tubercle was centered in the center of the Novel® matrix, characterized by the cross of the two main thicker lines.
- *Hip*: the subject is placed in a way that the greater trochanter is centered in the Novel® matrix, characterized by the cross of the two main thicker lines.
- *Knee*: the subject is placed in a way that the lateral meniscus is centered in the Novel® matrix, characterized by the cross of the two main thicker lines.
- *Heels*: the subject has been placed in such a way that the lateral malleolus is centered in the Novel® matrix, characterized by the cross of the two main thicker lines.

The tests consists in the recording of 4 areas for the supine and 4 areas for the lateral condition; for each area, a session has been recorded with the Novel® matrix after the DCPressure completed the Initialization phase, to be used as a baseline. During this phase, the subject has been let accommodate in the selected position for one minute before starting the recording. The baseline recording time was intially set as 5 minutes, but later changed to 2 minutes, due to the static situation considered. This data observation suggest that this consideration in the static data acquisition doesn't produce any loss of information.

After the baseline recording, a synchronized recording session between the Novel® pressure sensor matrix and the DCPressure mattress is started, through the Run mode in the DCPressure software.

The acquisition time was of 10 minutes for each area, for every subject, in each condition.

A schematic sequence of the protocol is reported below:

1. The mattress is inflated at the optimal standard setpoints through the Initialization mode on the DCPressure software.
2. After the internal pressions of the mattress cells are in the setpoints range, the patient is positioned in the desired location, respecting the guidelines mentioned above and is let

accomodate in place for one minute before starting the baseline recording. It is important that the subjects is wearing light clothes, to avoid any point of localized pression peaks.

3. After a minute, the baseline is recorded with the Novel® pressure sensor matrix, for a period of 2 minutes with a sampling frequency of 1 Hz. A light plastic sheet is positioned between the matrix and the patient in this phase, to avoid direct contact of the sensors with areas of clothing that could damage them.
4. The baseline recording is stopped and the actual efficacy recording test starts. At the same time, a recording with the Novel® matrix and the Run mode on the DCPressure matrix are started. The total acquisition time for this session is of 10 minutes, selecting a Novel® matrix sampling frequency of 1Hz.

The total number of acquisitions for this test are a baseline and an actual recording of the active mattress for each subject, for each condition. We considered two subjects in this test and two conditions (supine and lateral), for a total of 16 couples of baseline-active mattress recordings.

#### 2.3.2.4 Partecipant selection

The test involved three subvjects different in gender, height and weight: the first one is a 26 years old, 89 Kg weight, 1.75 m height male, the second one is a 25 years old, 50 Kg weight, 1.65 m height female and the third a 29 years old, 85 Kg weigth, 1.82 m height. All the subjects are in good health and have no posture problems that could affect the test results. During the data recording, care was taken that all wore light clothing that did not have areas capable of creating localized pressure peaks. All the data regarding the subjects are reported in *Tab. 1*.

	<i>Weight [Kg]</i>	<i>Height [m]</i>	<i>Age</i>
<i>Subj. 1</i>	89	1.75	26
<i>Subj. 2</i>	50	1.60	25
<i>Subj. 3</i>	85	1.82	29

*Tab. 1 – Partecipant information summary table.*

### 2.3.2.5 Long-term test

To understand the behaviour of the system in the long period, a test for a prolonged time was proposed. A non-uniform weight of 30 kG is placed on the mattress in the thoracic area, involving 16 cells, for a time of 16h. The mattress is set on run mode and the data of internal pressure of the interested cells are analyzed, using as reference the internal pressure of a cell in the same area but not loaded. A representation of the area interested and the reference cell is in *Fig. 25*.

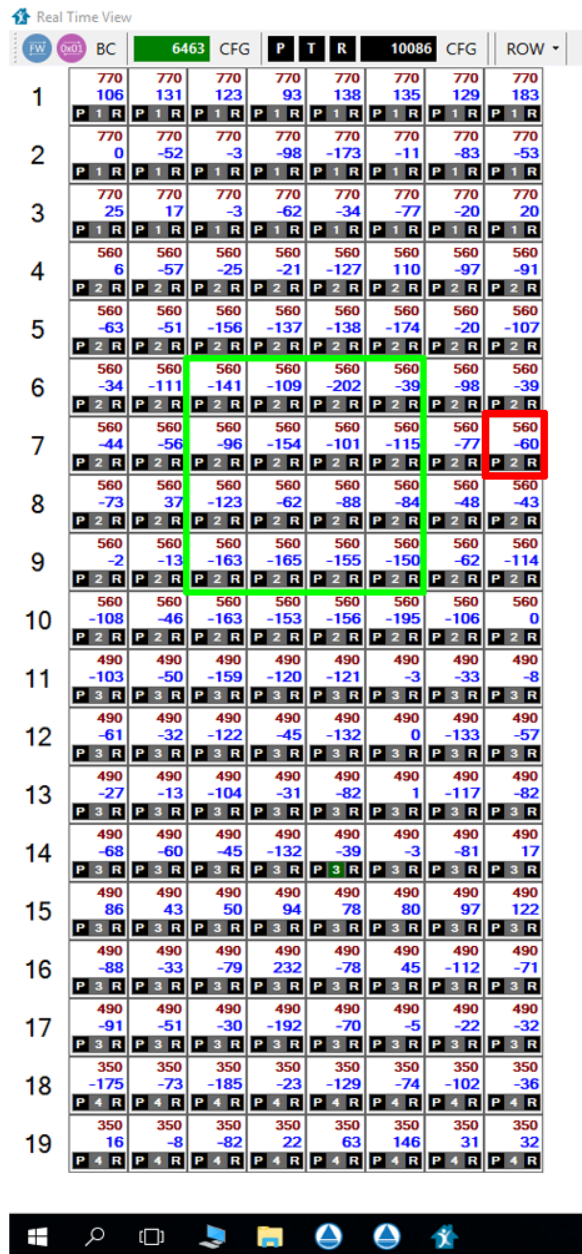


Fig. 25 – In green the positioning of the load, while in red the unloaded cell used as reference.

### 2.3.2.6 Data Description

The data coming from the Novel® pressure sensor matrix presents two different files: an ascii file containing the contact interface pressure measured by each sensor [kPa], presented in rows at each time interval, depending from the selected sampling frequency, 1 Hz in our case. The sensors are scanned simultaneously and reported starting from the sensor in the top left (Q16) to the one in the bottom right corner of the matrix (A1). In the file we can also find the file name given by the user through the Pilance software, the total acquisition time [s] and the peak pression [kPa\*s] and force time integrals [N\*s].

The .fgt file contains info about the total force [N] acting on the matrix and the x and y displacement [mm] of the center of pression (COP).

The data coming from the Run mode of the DCPressure mattress are .dat file that contains all the recordings made in a certain hour, synchronized with the PC clock. The data report a sequence of rows, containing in the first element a Timestamp value of the row and all the pression values of the cells in that period of time. Unfortunately, the data of the DCPressure cells are recorded with an irregular sampling frequency, that varies from 20 seconds to 1 minute. This is due probably to the processes of reading of the internal cells pression values, comparison with the setpoints and with the adjacent cells and inflation and deflation processes that must be activated to regulate the system. Another aspect that could be improved is the fact that all the recordings of the Run mode started in a determined hour are registered in the same file. This choice was made to optimize the space available for saving data.

### 2.3.2.7 Data processing

All the data have been processed with custom implemented Python scripts. Starting from the acquired data, for the Novel® pressure sensor matrix, the data are reported as a matrix with 156 columns, one for each sensor and a row for every data recorded, one for each second in our case, choosing a sampling frequency of 1 Hz. Selecting a different number of rows of this initial file allow us to consider only partial frames, performing a time selection, while selecting different rows allow us to select only specific sensors of the matrix, performing a spacial selection. Of course the

two selections can be combined to have the data of selected cells in selected moments or intervals of time.

The first process consists in the spacial correlation between the data obtained by the Novel® sensor matrix and the ones by the mattress. In this step, the definition of a standard positioning among the different subjects and the positioning of the matrix in standard positions for each body location, allowing to know this correspondence for each test. As output measures the maximum presion [kPa] and mean pression are reported. In this phase, only the active sensors have been considered, to calucate the pressure values only in the active area and not on the overall matrix (i.e. Fig. 26).

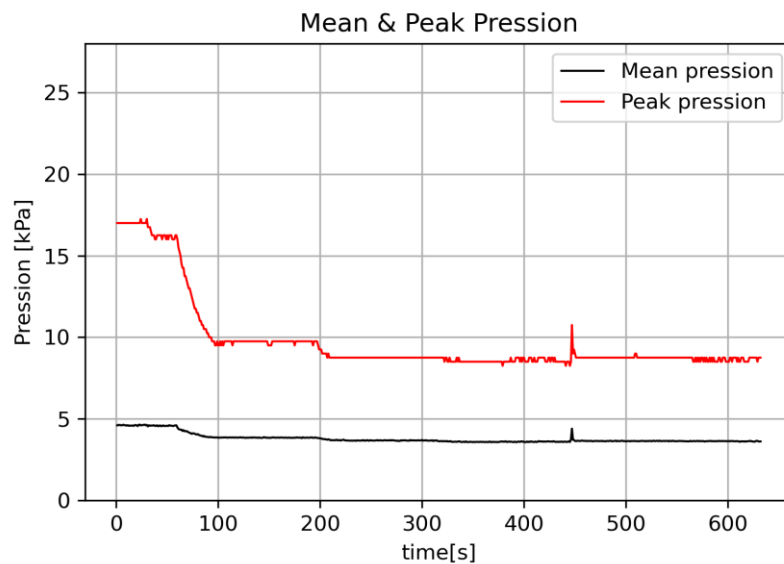


**Fig. 26** – Mean (black) and maximum (red) pressure [kPa] recorded by the Novel® matrix.

Knowing the extension of a single cell, that is 6,003 cm<sup>2</sup>, it is possible to know the active area, multiplying this factor by the total number of active sensors for each time instant (Fig. 27).

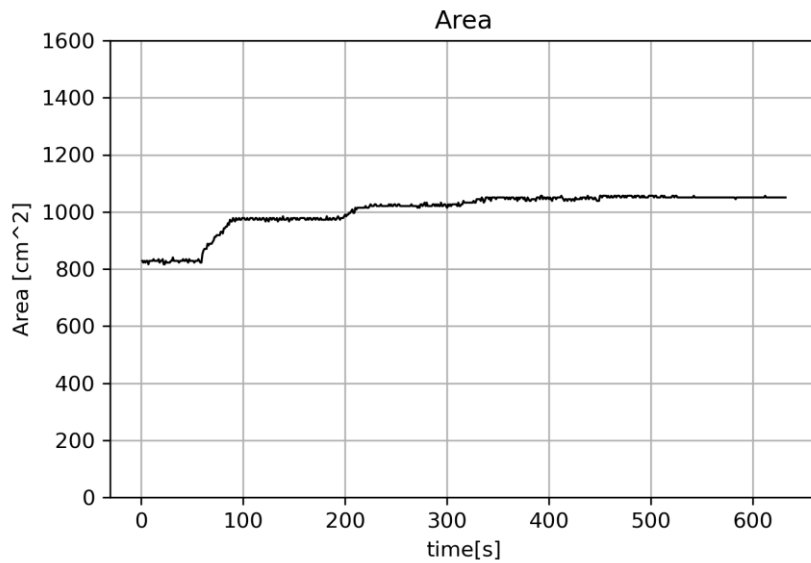


**Fig. 27** – Novel® matrix active area [cm<sup>2</sup>] interested, calculated as the number of active sensor at each time instant by the area of a single sensor.

In a similar way it is possible to find how many sensors recorded a pressure value over the threshold that is, in our case 30 mmHg (4 kPa). Comparing this value with the total number of active sensors in that instant, it is possible to express in percentage how many active sensors are over the threshold for each instant (*Fig. 28*).

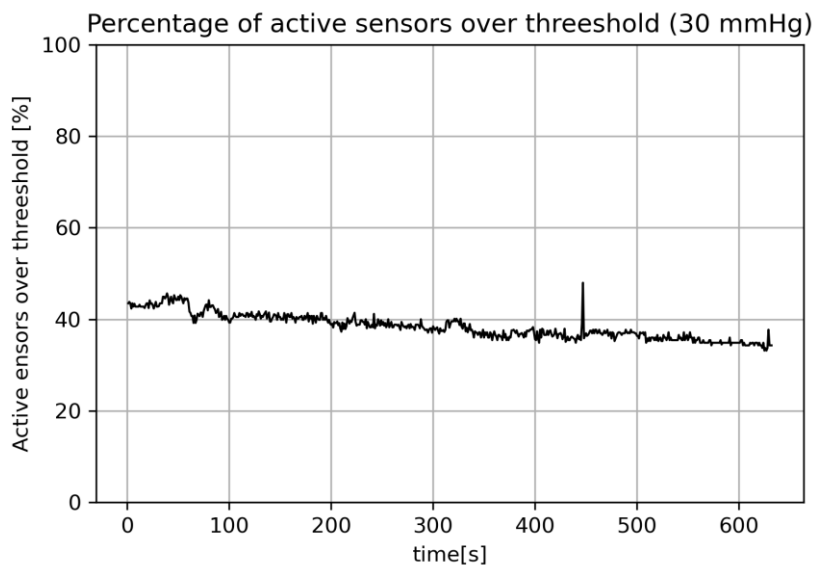


**Fig. 28** – Percentage of active sensors that overcome the 30 mmHg threshold.

Once the values of pressure and the area are known, the total force [N] acting on the area can be found (Fig. 29).

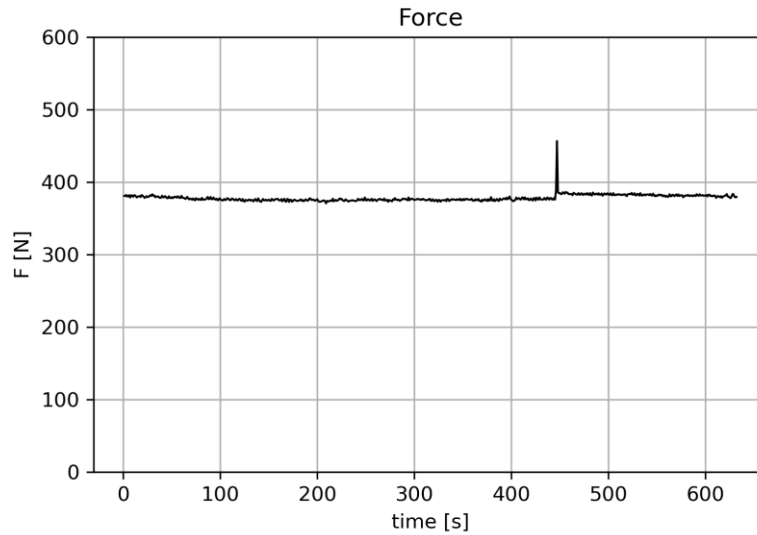


**Fig. 29** – Force [N] that is exerted on the active area of the Novel® matrix, calculated multiplying the total pressure on the matrix by the active area for each time instant.

Regarding the data coming from the DCPressure mattress, remodelling the data with correct timestamp data conversions, it is possible to obtain the information about the air chamber internal pressure evolution in time (Fig. 30).

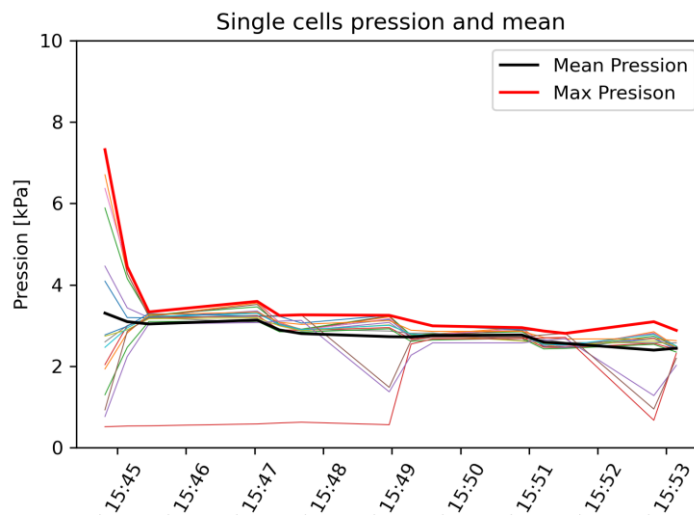


**Fig. 30** – Mean and maximum pressure of the 16 cells under the Novel® pressure matrix time evolution.

The spacial association between the values contained in the Novel<sup>®</sup> matrix and the data coming from the DCPressure can be done through the scheme reported in *Fig. 24*. It is important to underline that the sampling frequency of the DCPressure mattress is not constant, and all the data recorded in a certain hour are saved in the same file, but thanks to the timestamp conversion it is possible to manually select the rows corresponding to the same time instants. All the values of mean and maximum pressure, both for Novel<sup>®</sup> and DCPressure can be reported to a simpler visualization using plots and colormaps found in the “Results” paragraph.

### **2.3.2.8 Calibration Curve**

The calibration of the device is not an easy task: many aspects involve the values recorded by the mattress cells in time, such as the mutual cells compression when loaded or the external perturbation given by the system during the inflation and deflation in the different phases of the system functioning. The behaviour that a cell has taken individually outside the mattress is different than the one that has when coupled in a tight space under the system control.

Furthermore, the different mattress area area inflated at a different initial setpoint pressure, and this aspect can change the behaviour of the cells when subject to load.

A solution to overcome these problems is considering the mattress in the first minute, in which the system controls acts marginally, only checking the patient positioning and the values of pressure are not altered by the system deflation of the cells. To avoid the effect of the different initial setpoints, it could be possible to evaluate not the absolute value recorded by the DCPressure mattress, but the difference between the actual value and the initial one, applying a corrective factor to the four groups and considering all in terms of variations from the initial condition and not as absolute value.

The results of these considerations are reported in the relative chapter in the “Results” paragraph.

### 3. Results

#### 3.1 Single cell stress test

The chamber internal initial pressure is for both tests 100 mbar. The results are reported in *Fig. 31* and *Fig. 32*, showing the graphs of the load [N] and internal pressure read on the analogic manometer [kPa], and the effects on the cells.

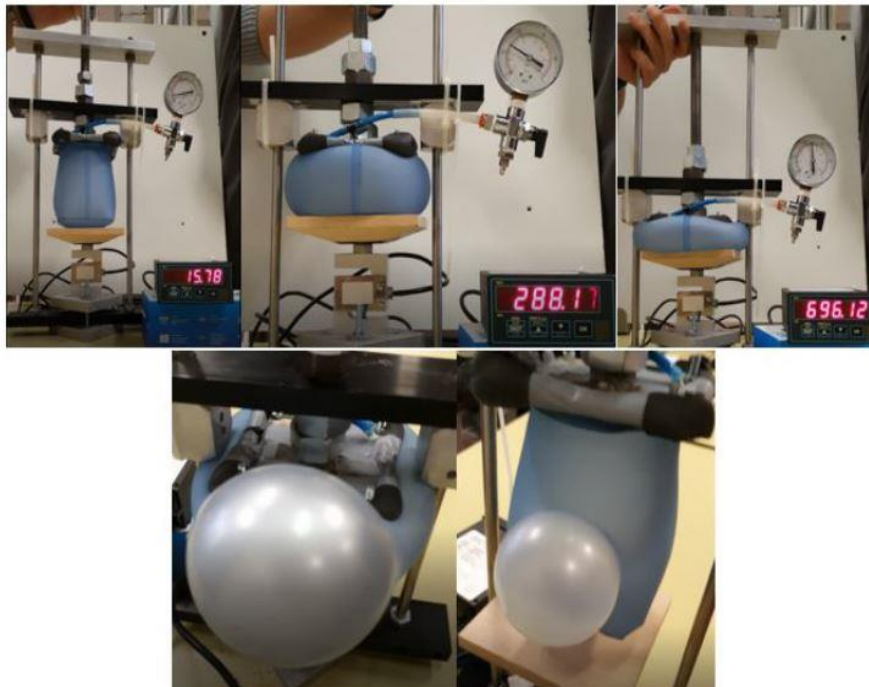
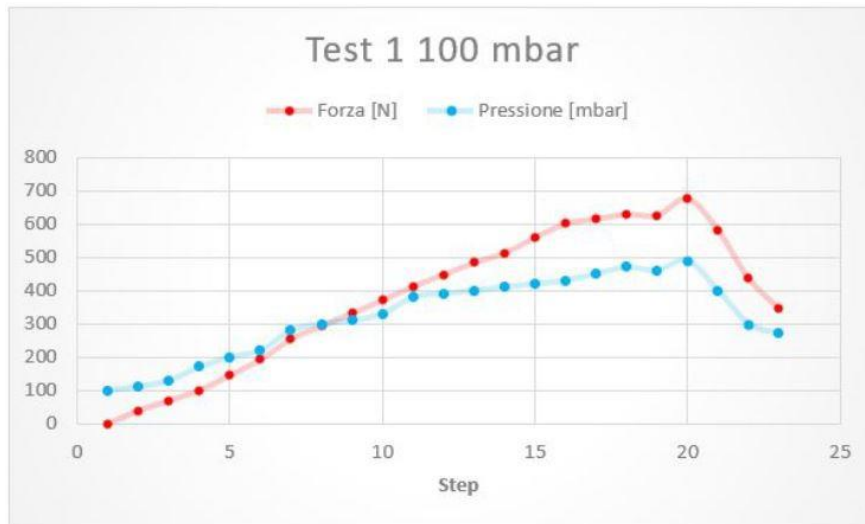


**Fig. 31** – In the upper image we find the graph of load exercised on the cell (red) and the internal pressure (blue). In the bottom image, some steps of the test; in particular the irreversible deformation of the cell.

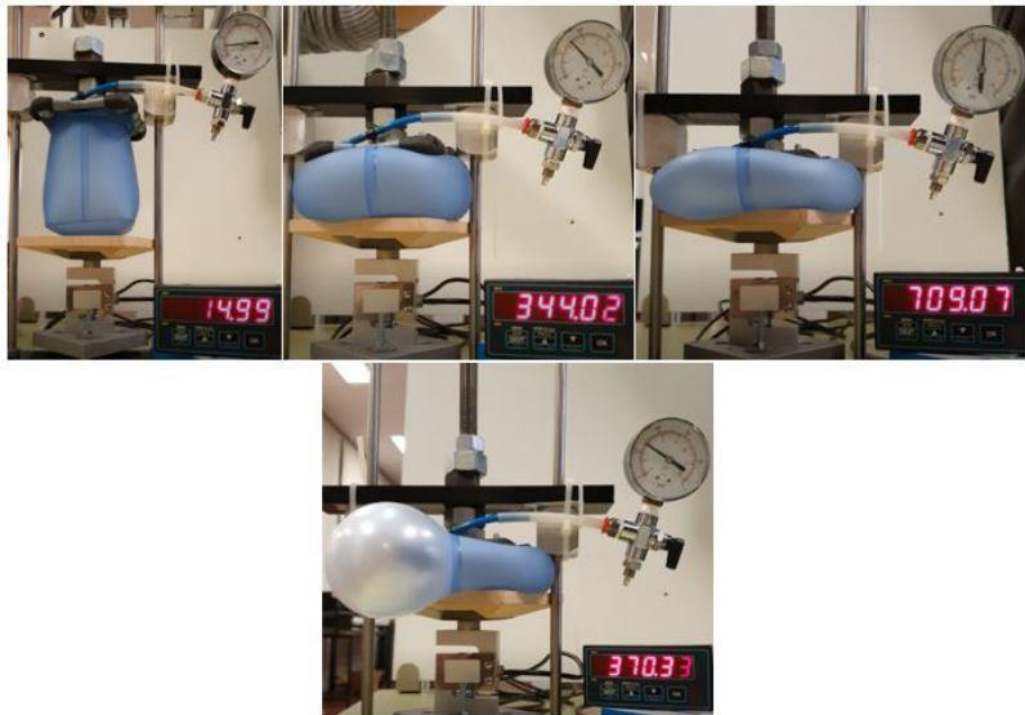
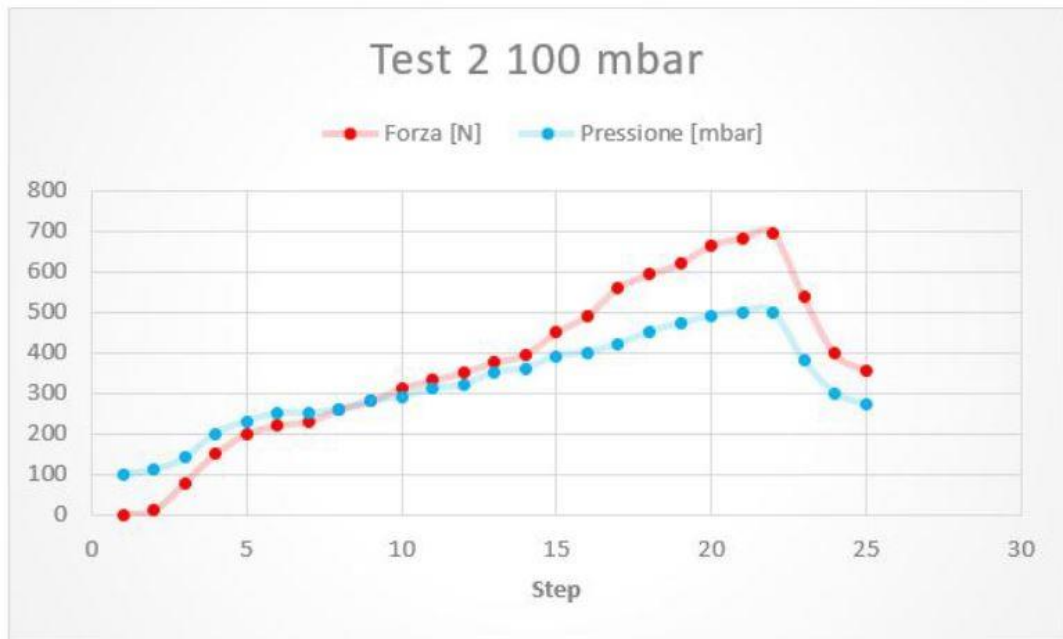


**Fig. 32** – Second test with the chamber internal pression at 100 mbar. The values are similar to the ones in the previous test and also in this condnition we have an irreversible deformation of the cell.

In the first test, the maximal load exercited before the internal pression falling, due to the cell deformation, is of 676 N, registering an internal pression of 490 mbar. In the second test, the maximal load registered is of 681 N at an internal pression of 500 mbar.

### 3.2 Single cells efficacy test

In Fig. 33, the maximum pression, expressed in kPa (1 Hz sampling frequency) recorded by the Novelx® matrix in the single cell efficacy test. The pression peak in the area, after the complete deflating of the cell, falls from values between 20 and 25 kPa to values between 7.5 and 10 kPa. In the figure also the mean peak pression values in the first 48 seconds (Before Deflation, B.D.) and in the last minute (After Deflation, A.D.) are reported, respectively in red and green.

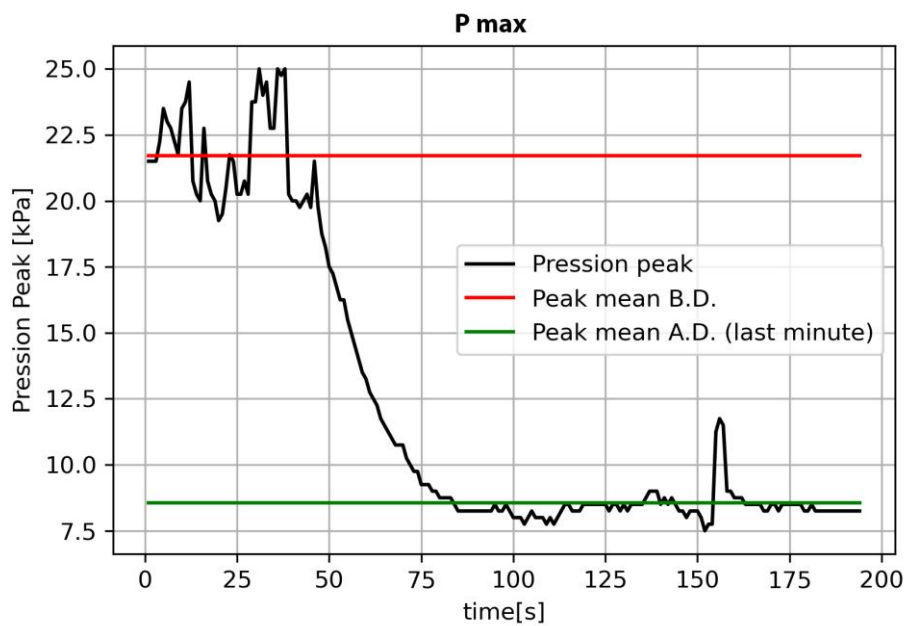


**Fig. 33** – In black, the maximum value registered by the Novel® matrix 4x4 cells array, corresponding to the greater trochanter. The corresponding mattress cell has been deflated after 48 seconds. The mean peak pression values in the first 48 seconds (Before Deflating, B.D.) and in the last minute (After Deflating, A.D.) have been reported, respectively in red and green.

From the data of the Novel® matrix, the mean values in the relative considered intervals of the single cells composing the 4 x 4 array are reported in Fig. 34, showing how the deflating of the mattress cell under the matrix causes a drop in the peak of the interface contact pression.

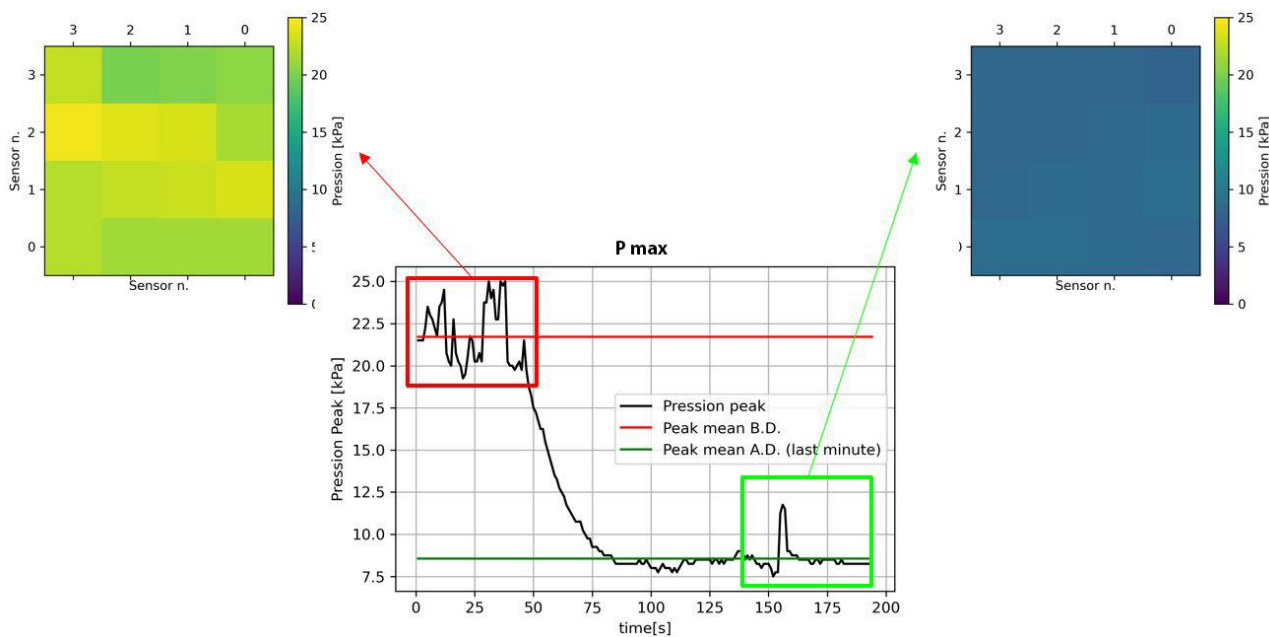


**Fig. 34** – In the center, the mean of the maximal pression values of the single cells composing the 4x4 Novel® matrix subset under the greater tubercle. Hightled in red, the mean in the first 48 seconds (B.D.) and in green in the last minute (A.D.), with the relative colormaps.

The exact values of mean maximal pression in the 4 x 4 cells, the one relative to the first 48 seconds, to the last minute and the improvement, expressed in kPa and percentage are reported in *Tab. 2*.

Max Pression [kPa]	Peak pression B.D. mean [kPa]	Peak pression A.D. (last 60 s) mean [kPa]	Mean peak variation [kPa]	Mean peak improvement [%]
25,00	21,70	8,56	-13,14	60,56

**Tab. 2** – Table relative to the deflating of a single cell under the greater tubercle of a 50 Kg, 1,65 m height, side-lying female subject on the DCPressure mattress. The values are relative to the values registered by the Novel® pressure sensor matrix in the interested mattress cell, respectively to maximal peak pression [kPa], its mean in the first 48 seconds, in which the mattress cell is not deflated (B.D.), the mean of the peak in the last 60 seconds (A.D.) and the variation between these two expressed in kPa and percentage.

### 3.3 DCPressure supine and lateral tests.

For the supine and lateral lying tests, we have a total of 4 positions considered for each condition, for each subject tested, for a total of 16 couples of baseline-recordings. For each recording, we can compare the parameters calculated in the chapter “Data Processing” between the mattress in the Initialization phase and during the Run mode. The parameters taken in consideration are:

- total force [N] over the Novel® matrix
- active area [cm<sup>2</sup>] of the Novel® matrix
- mean pression [kPa] over Novel® matrix
- peak pression [kPa] over the Novel® matrix
- Percentage [%] of Novel® matrix sensors over the 30 mmHg threshold
- mean pression [kPa] of the mattress cells relative to the interested area
- peak pression [kPa] of the mattress cells relative to the interested area
- colormap of the mean pressure distribution in the Novel® matrix
- colormap of the mean pressure distribution in the corresponding mattress cells
- colormap of the mean pressure distribution in the overall mattress

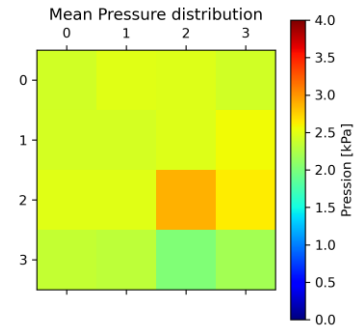
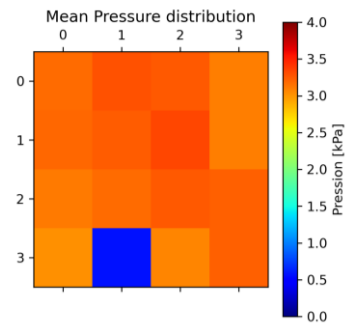
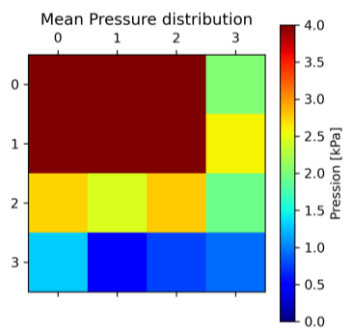
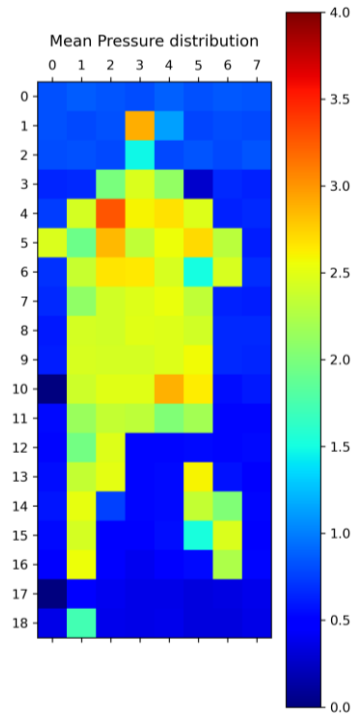
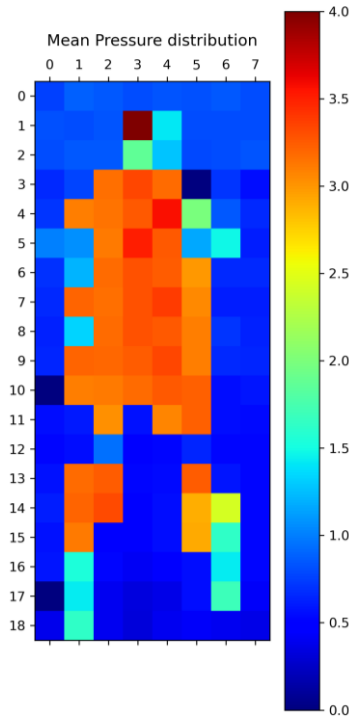
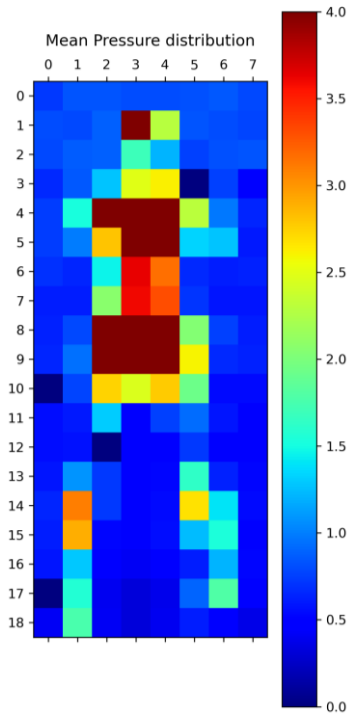
In the following section is reported an example of the processed outputs relative to the recordings of the hip of the first subject in supine position and the shoulder of the second subject in the lateral position.

Subject 1 – Supine lying – Hip

1<sup>st</sup> min

2<sup>nd</sup> min

10<sup>th</sup> min



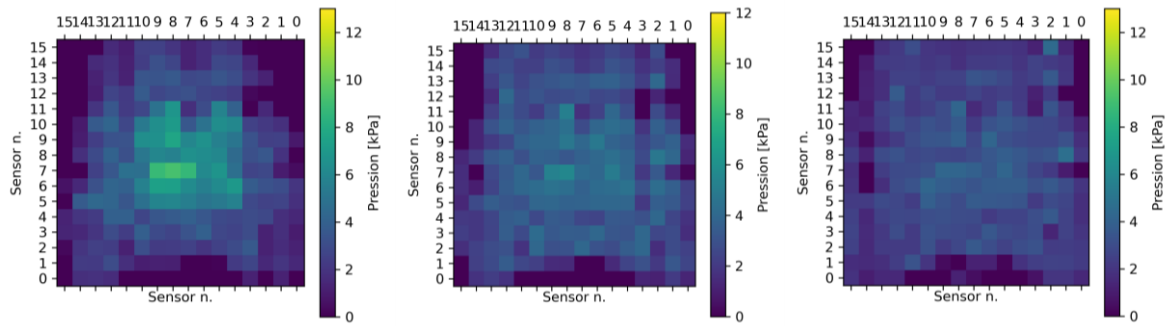


**Fig. 35** – Mean pressure [kPa] values of the subject 1 hip test in supine position. On the top row, the mattress mean pressure values relative to the 1<sup>st</sup>, 2<sup>nd</sup> and last minute. On the second row, the same plots focused in the hip area and in the last row, the colormaps in the same intervals, relative to the mean values for each sensor of the Novel® matrix.

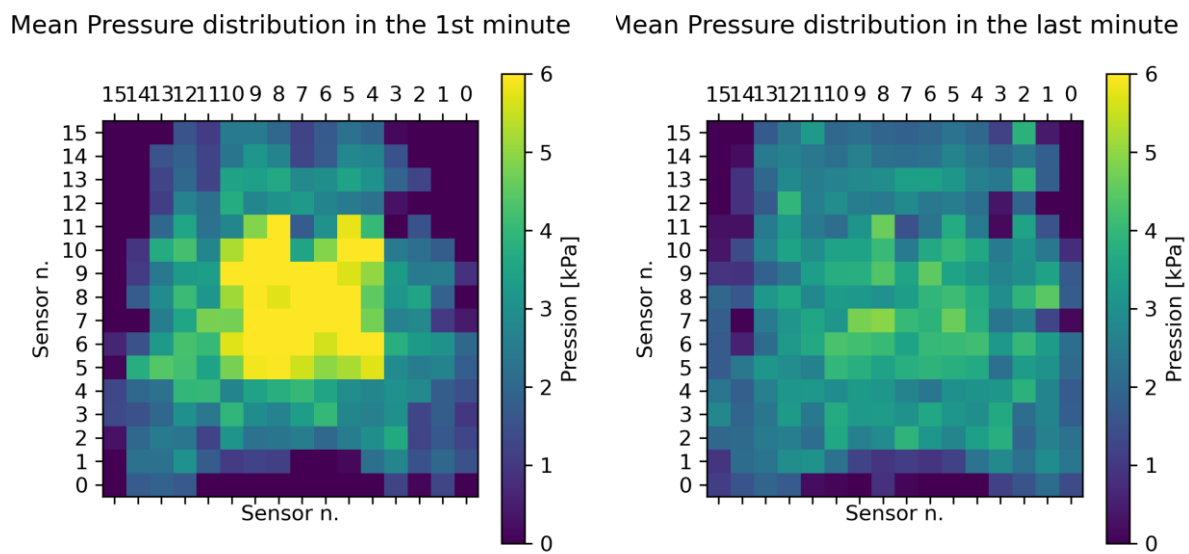


**Fig. 36** – 2D representation of the mean pressure in the first and last minute of the pressure on the Novel® matrix of subject 1 hip, lying in supine position during the mattress activity test.

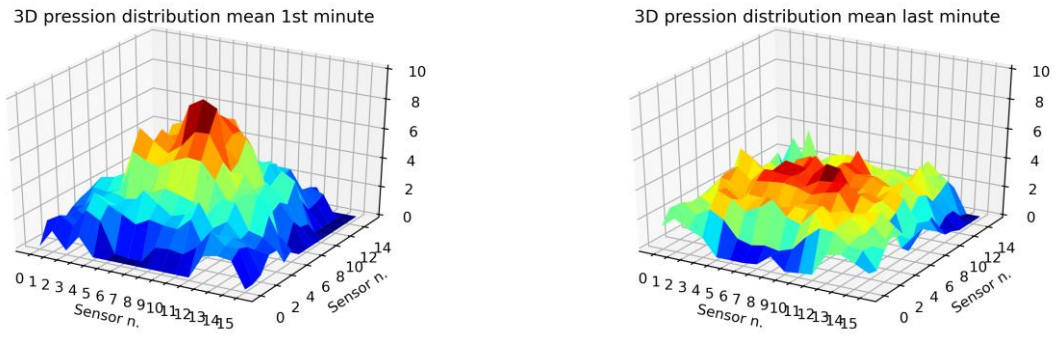


**Fig. 37** – 3D representation of the mean pression distribution on the Novel® platform of the hip of subject 1 lying supine, in the first minute of mattress activity and in the last one.

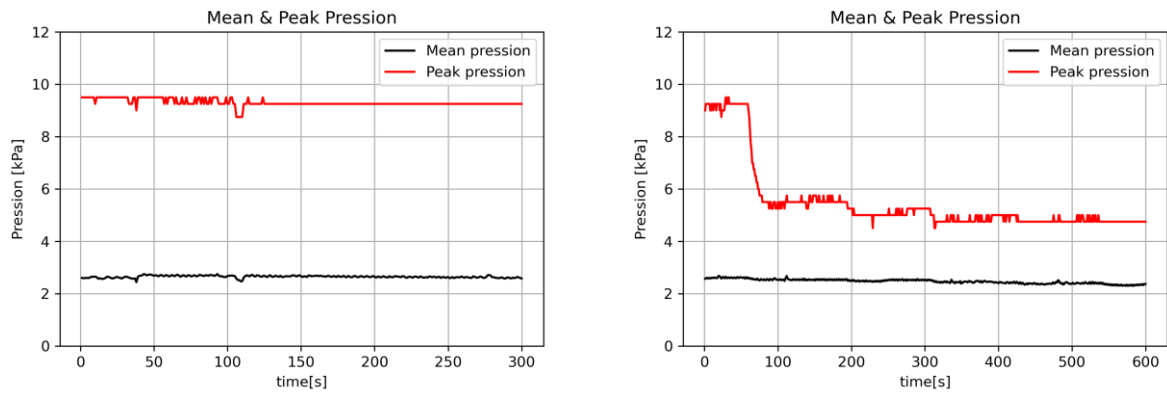


**Fig. 38** – In red we find the peak pression [kPa] registered by the Novel matrix over time, while in black the mean pression [kPa]. The left image is relative to the baseline, while the right one to the DCPressure Run mode.

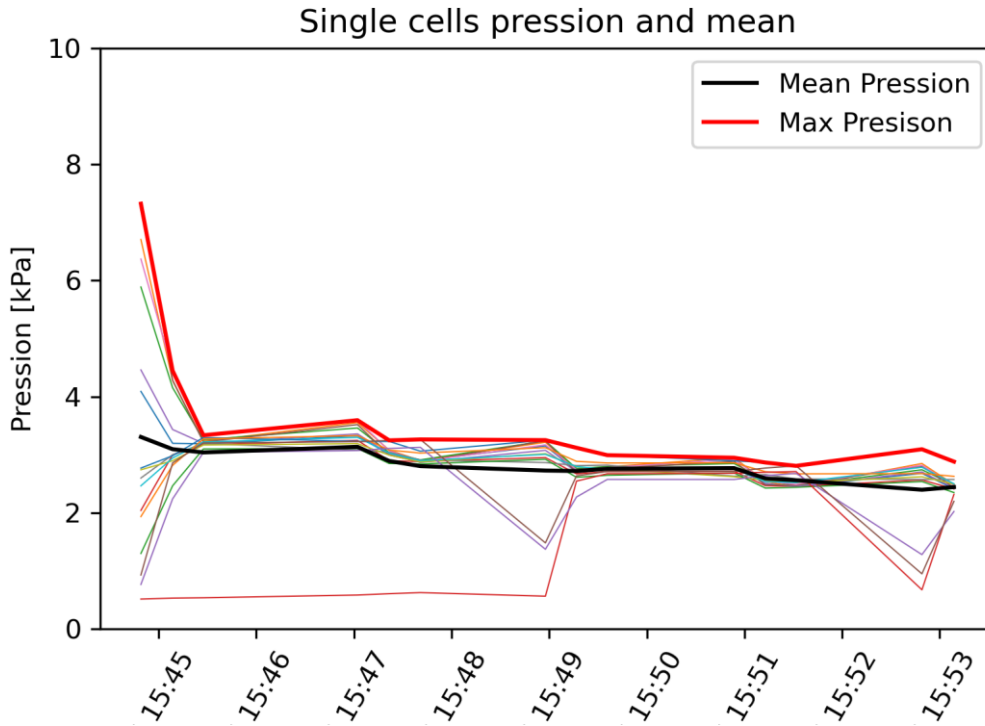


**Fig. 39** – Internal pressure [kPa] values of the DCPressure 16 cells in the interested area, the hip in this case. In red we find the maximal pression, while in black the mean pression.

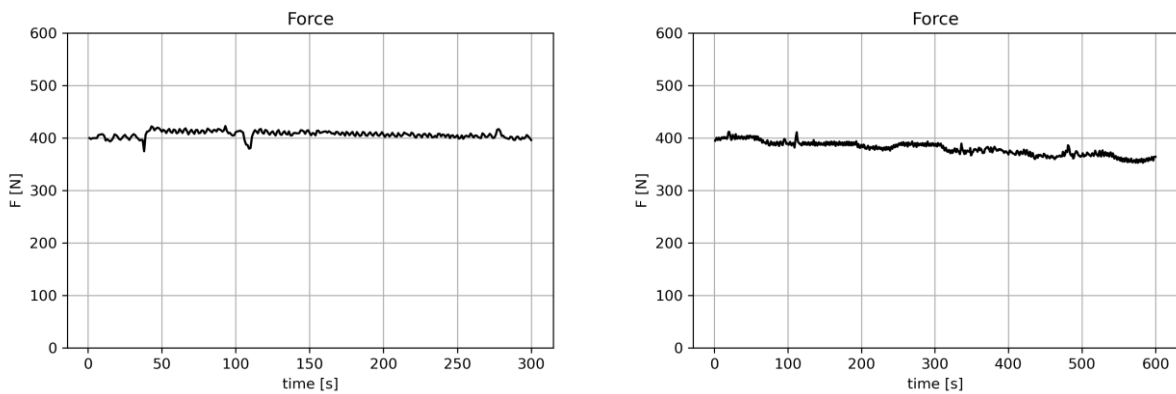


**Fig. 40** – Interface contact force trend in time of the subject 1 hip. On the left the 3 minunte long baseline, recorded by the Novel® pressure matrix after the DCPressure mattress was initialized and the cells borught at the setpoint values. On the right, the same values recorded after the Run mode of the DCPressure is started.

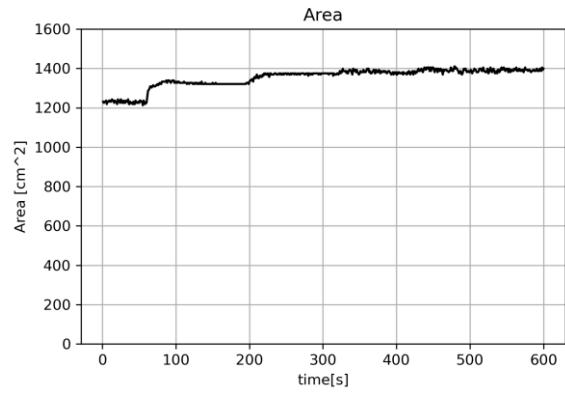
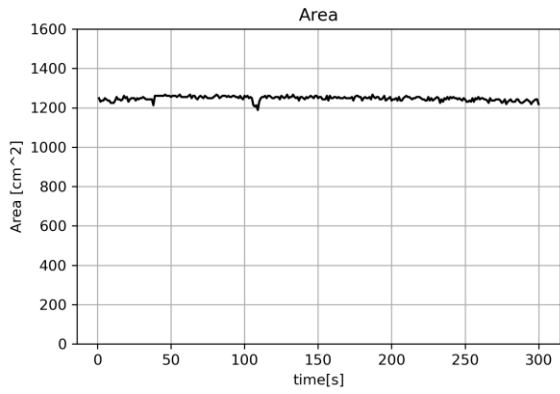


**Fig. 41** – Area [cm<sup>2</sup>] calculated by the Novel matrix values. On the left, the recordings relative to the baseline, while on the right the ones relative to the DCPressure Run mode.

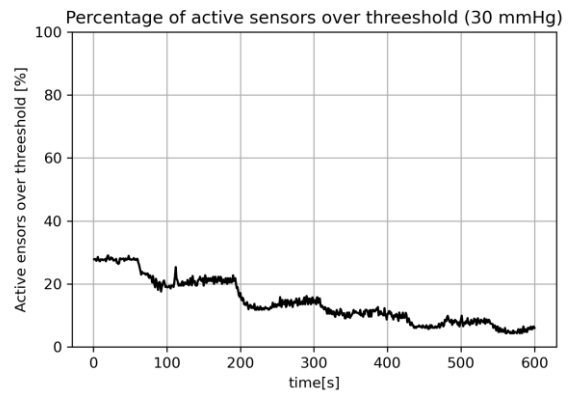
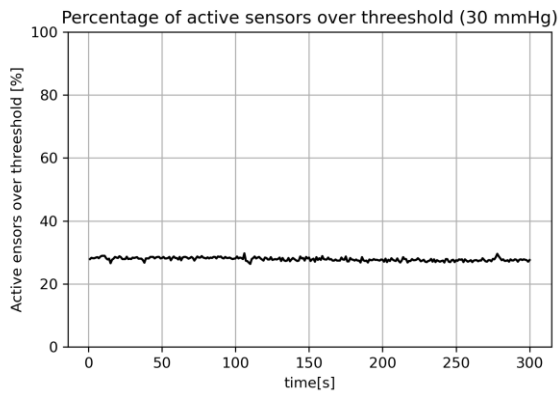


**Fig. 42** – Percentage [%] of Novel<sup>®</sup> sensors over the 30 mmHg threshold. In the left, the values relative to the baseline, while in the right the values of the DCPressure Run mode.

Subject 2 – Lateral lying – Shoulder

1<sup>st</sup> min

2<sup>nd</sup> min

10<sup>th</sup> min

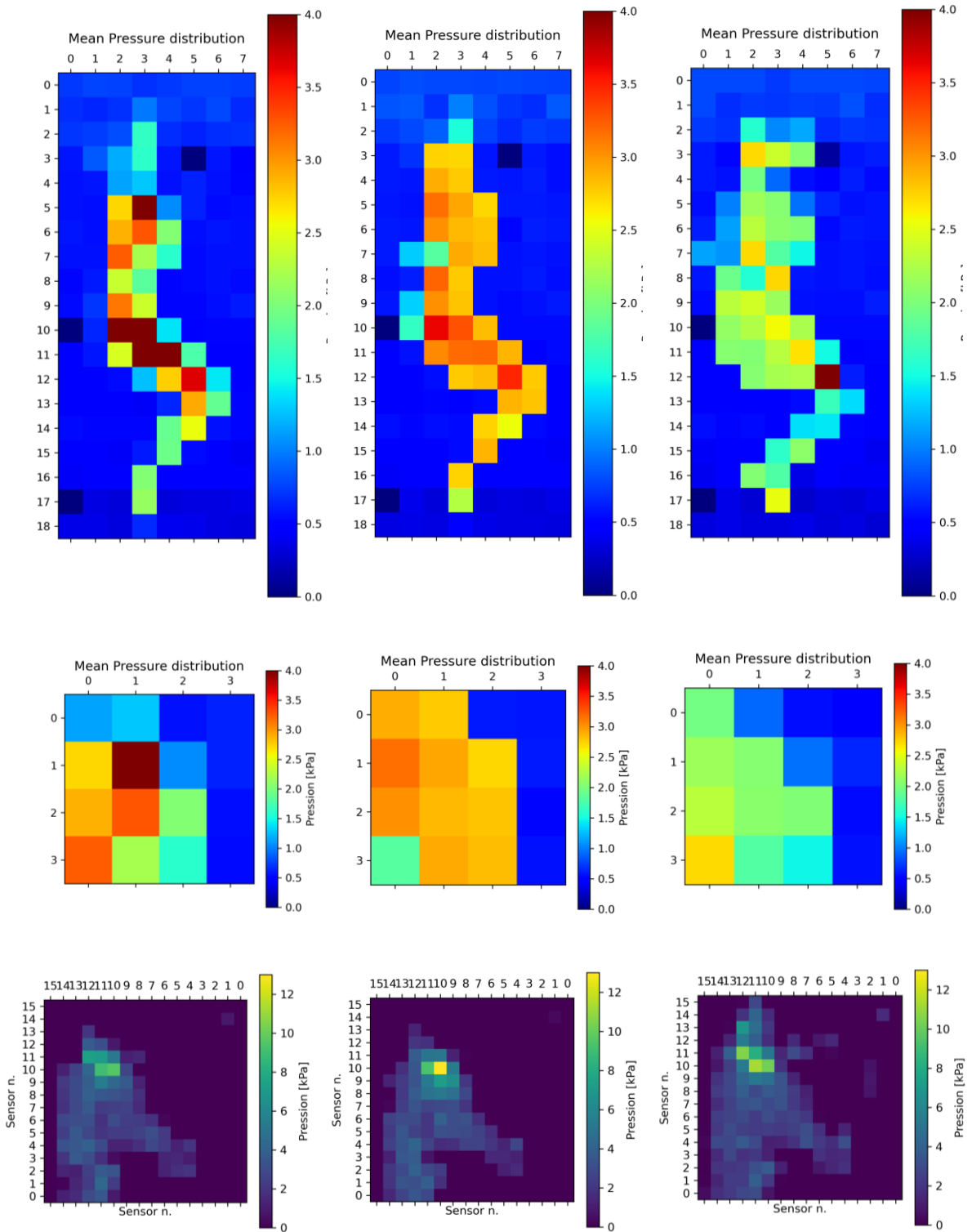
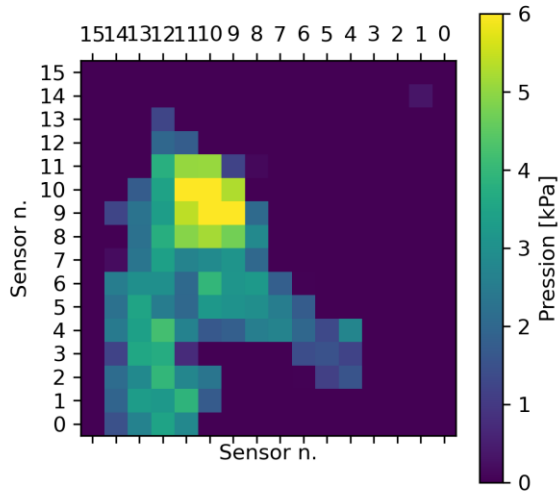


**Fig. 43** - Mean pressure [kPa] of the subject 2 shoulder test in lateral position. On the top row, the mattress mean pressure values relative to the 1<sup>st</sup>, 2<sup>nd</sup> and last minute. On the second row, the same plots focused in the hip area and in the last row, the colormaps in the same intervals, relative to the mean values for each sensor of the Novel<sup>®</sup> matrix.

Mean Pressure distribution in the 1st minute



Mean Pressure distribution in the last minute

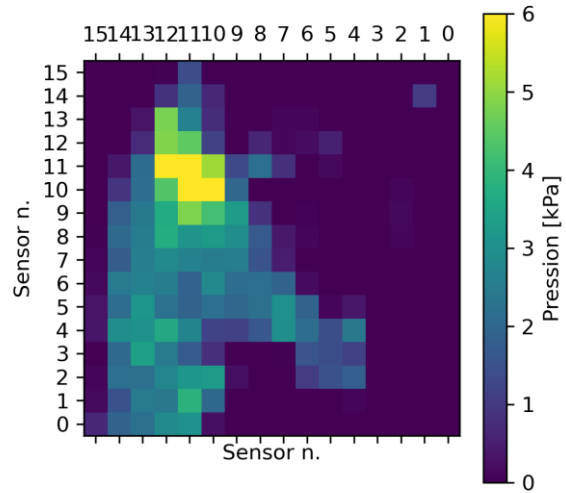
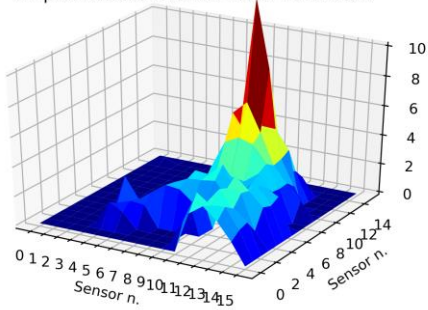


**Fig. 44** – 2D representation of the Novel® pression mean minute of the shoulders of subject 2 lying lateral in the first and last minute of mattress activity test.

3D pression distribution mean 1st minute



3D pression distribution mean last minute

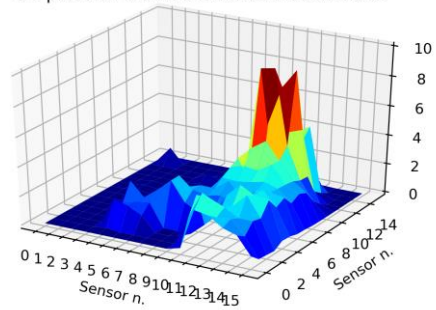


**Fig. 45** - 3D representation of the mean pression distribution on the Novel® platform of the shoulders of subject 2 lying lateral, in the first minute of mattress activity and in the last one.

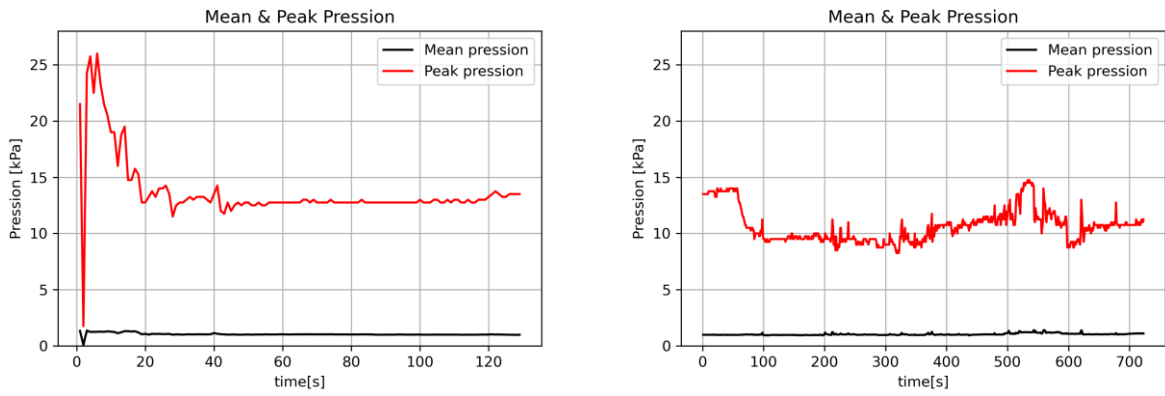


**Fig. 46** – In black the mean pressure [kPa] and in red the peak pressure [kPa] registered by the Novel® matrix for the test relative to the shoulder of subject 2 in lateral position. In the left the baseline recording, while in the right the actual test with the Run mode of the DCPressure mattress.

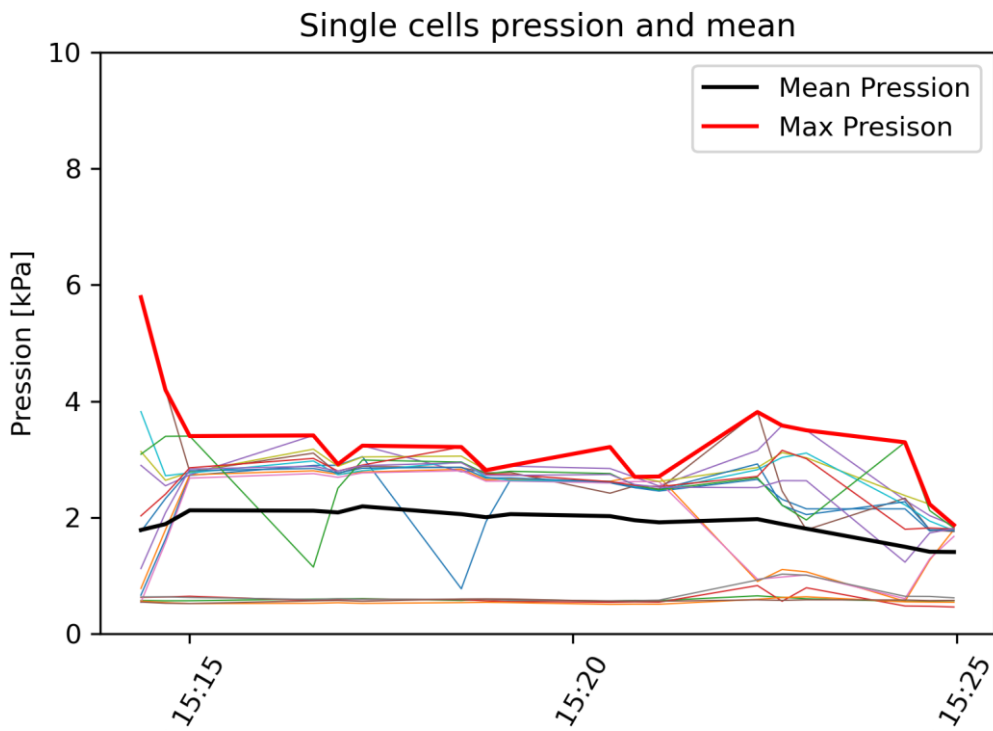


**Fig. 47** – Internal pression values [kPa] of the 16 DCPressure mattress cells relative to the interested area during the Run mode. In red the peak pression and in black the mean value.

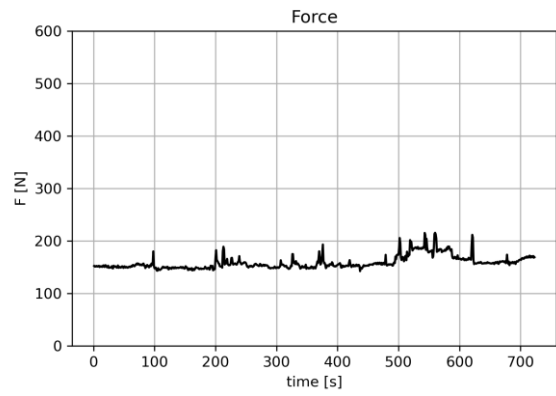
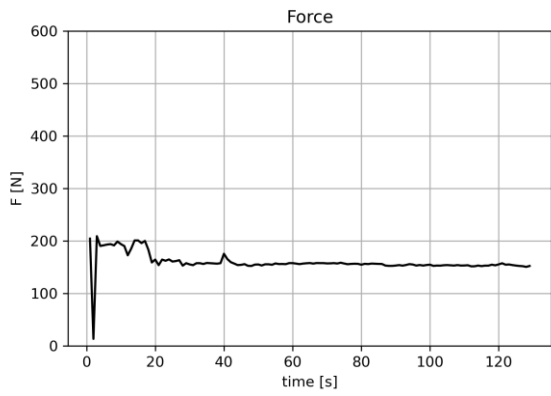


**Fig. 48** – Force [N] time evolution on the Novel® matrix, relative to the subject 2 shoulder in lateral lying position. On the left, the image relative to the baseline, while on the right the one relative to the DCPressure Run mode.

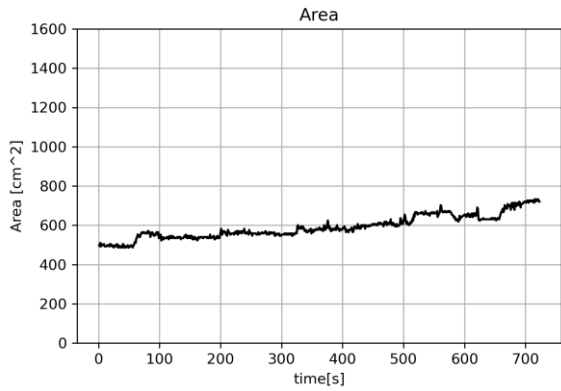
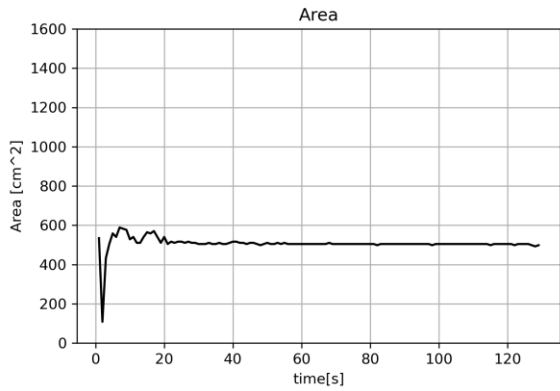


**Fig. 49** – Area [cm<sup>2</sup>] of the Novel® matrix recruited in the test of subject 2 shoulder. On the left, the image relative to the baseline, while on the right the one of the DCPressure run mode.

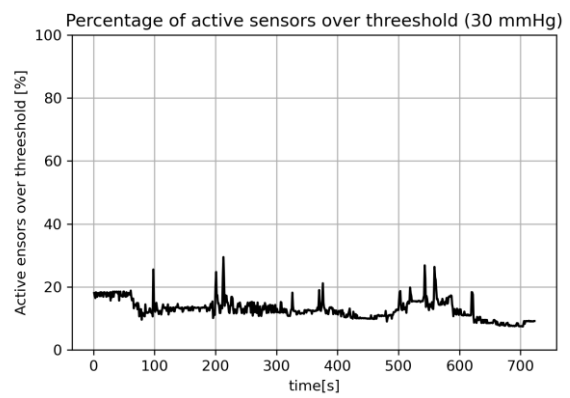
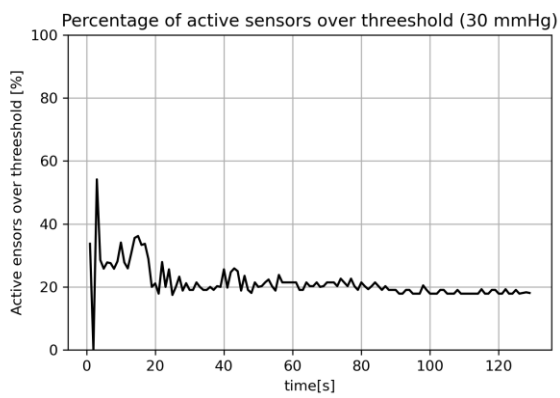


**Fig. 50** – Percentage [%] of Novel® sensors over the threshold of 30 mmHg. On the left, the values relative to the baseline, while on the right the ones to the DCPressure Run mode.

From the images reported above, it is possible to affirm that the mean pressure values in the first minute of mattress activity are comparable with the ones of the mattress turned off, meaning that the activity of the device starts after one minute. Knowing this, it is possible to use the data collected in the first minute of the mattress activity as a baseline and a comparison value to assess the efficiency of the mattress. The main factors we are interested in is the reduction of mean contact interface pressure, the area and the number of sensors that overcome the 30 mmHg threshold. While the first can be calculated as the difference between the mean value of mean pressure on the active area in the last minute minus the one in the first minute, for the latter is important to know also not only the percentage of sensors that register a value over the threshold, but also compare this number with the total number of active sensors. Indeed, during the mattress activity the area increases, as we can see from the figures above, because the contact interface area increases due to the deflation of the mattress cells beneath. So, we reported also the area increase, calculated as the difference between the interested area in the last minute minus the one in the first one, and the percentage of sensors over threshold has been divided by the total number of active sensors. For example, if we have at the end a percentage of 5% of over-threshold sensors, on a total of 31 active sensors in the last minute, is different than having 5% of over-threshold sensors on a total of 24 active sensors in the first minute. The measures relative to the parameters described above are reported for each body location and for each condition in the *Tab. 2*.

Body Part	Subject n.	$\Delta P_{\max}$ [kPa]	$\Delta P_{\max}$ [%]	$\Delta$ Area [cm <sup>2</sup> ]	$\Delta$ Area [%]	$\Delta$ ots/ns
Head Supine	1	-0,50	-17,06	41,16	28,04	-0,05
	2	-0,06	-2,27	22,93	10,85	0,00
	3	0,05	1,44	-4,91	-3,95	-0,03
Shoulders Supine	1	-0,71	-22,05	180,92	19,07	-0,32
	2	-0,65	-28,02	137,76	36,65	-0,05
	3	-0,94	-25,97	135,51	17,83	-0,36
Shoulders Lateral	1	-0,44	-12,87	83,19	9,96	-0,20
	2	-0,38	-12,46	104,18	21,04	-0,06
	3	-0,65	-16,75	205,04	27,76	-0,20
Hip Supine	1	-0,49	-15,03	136,81	11,13	-0,15
	2	-0,96	-30,48	177,63	25,43	-0,27
	3	-1,19	-29,38	316,77	36,02	-0,29
Hip Lateral	1	-0,93	-20,71	91,13	10,28	-0,12
	2	-0,88	-24,18	161,77	26,44	-0,15
	3	-0,89	-19,39	194,33	23,47	-0,06
Knee Lateral	1	0,08	2,60	34,50	6,22	-0,07
	2	-0,35	-11,18	58,33	12,54	-0,17
	3	-0,22	-7,51	10,48	2,25	-0,13
Feet Supine	1	-0,01	-0,49	-6,80	-3,66	0,07
	2	-0,20	-8,37	-21,40	-10,97	-0,02
	3	-0,91	-22,20	16,62	9,02	-0,11
Feet Lateral	1	0,06	2,60	-9,54	-4,80	0,00
	2	0,20	11,63	7,55	6,28	0,00
	3	0,20	7,63	9,04	5,77	-0,05

**Tab. 2** – Difference in pression (expressed in kPa and %), area (expressed in cm<sup>2</sup> and %) and over-threshold sensors in relation to the total number of active sensors between the last minute and the first minute of mattress activity in the 10 minutes tests for each body area of each one of the three subjects.

As we can see from the table, we can find a significant reduction in the mean contact interface pressure recorded with the Novel® sensor matrix, as we can appreciate also from the trends in Fig. 37. In order to have a better visualization of these differences and also to appreciate the different behaviour and effectiveness  $\Delta P$  depending on the weight that the mattress has to redistribute, all the measures relative to the single body parts of the subject above have been grouped in a more compact Tab. 3.

		$\Delta P_{\max}$ [kPa]	$\Delta P_{\max}$ [%]	$\Delta$ Area [cm <sup>2</sup> ]	$\Delta$ Area [%]	$\Delta$ ots/ns [%]
Head	Mean	-0,17	-5,97	19,73	11,65	-0,03
	SD	0,29	9,79	23,20	16,01	0,03
Shoulders	Mean	-0,63	-19,69	141,10	22,05	-0,20
	SD	0,20	6,66	45,68	9,16	0,13
Hip	Mean	-0,89	-23,19	179,74	22,13	-0,17
	SD	0,23	5,99	76,17	9,86	0,09
Knee	Mean	-0,16	-5,36	34,44	7,00	-0,12
	SD	0,22	7,14	23,93	5,19	0,05
Feet	Mean	-0,11	-1,53	-0,76	0,27	-0,02
	SD	0,42	12,24	14,19	7,88	0,06
Total	Mean	-0,45	-12,52	86,79	13,44	-0,12
	SD	0,42	12,23	88,44	12,95	0,11

**Tab 3** – All the data coming from the same body location have been grouped among all the subjects and the supine and lateral tests. This introduces wide errors, due to the different lying of the subjects and also the their difference in weight, but still allows to appreciate the difference in performance of the mattress regarding the different weight that is put on it.

This visualization introduce high errors, due to the different ways of lying that are however grouped together and the already wide difference in body weight of the subjects, but still allow us to appreciate the different mattress performances outcomes in relation to the weight that must be redistributed. The results of *Tab. 3* are better visualized in the following graphs, showing the difference in pressure, expressed in absolute value [kPa] and percentage, the increasing in the areas, also expressed in cm<sup>2</sup> and percentage, and the percentage of over-threshold sensors in relation to the total number of active sensos for each body location.

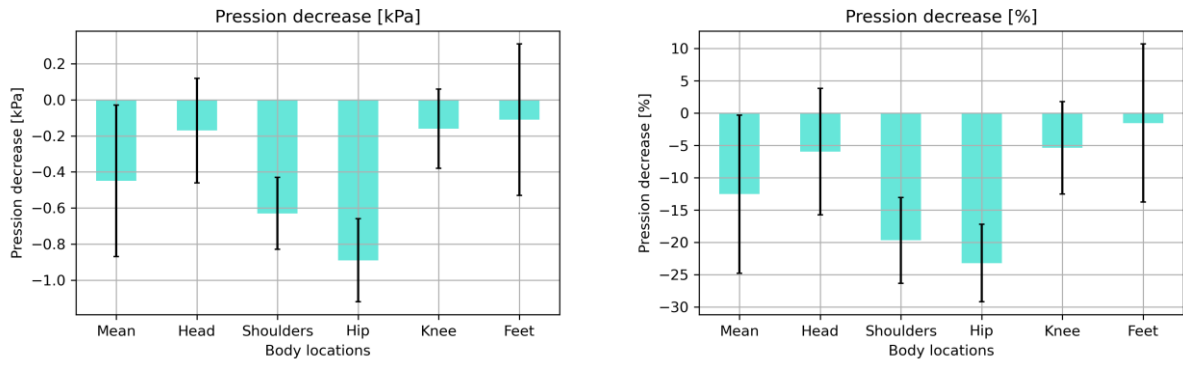


**Fig. 51** – Decrease of pressure registered by the Novel® platform between the last and first minute of mattress activity, expressed in kPa and %, for each body location.

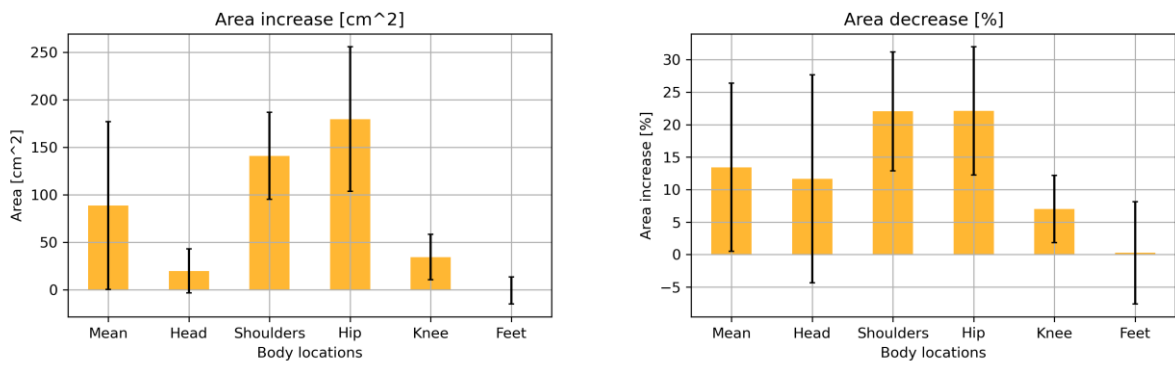


**Fig. 52** – Increase in the area of the Novel® matrix between the last and first minute of mattress activity, expressed in cm<sup>2</sup> and %, for each body location.

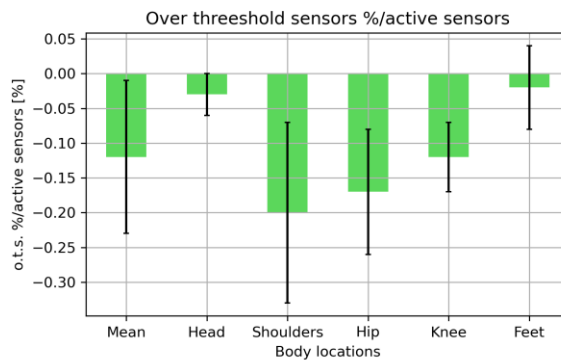


**Fig. 53** – Decrease of over-threshold sensors, normalized respect to the total number of active sensors, between the last and first minute of mattress activity, for each body location.

Another way to assess the efficacy of the mattress regarding the weight that is taken in consideration, is to group the results of *Tab. 3* by mass intervals. The weight of the body part taken in consideration has been calculated as the mean force exercised on the Novel® matrix in the first 10 seconds of baseline recording, divided by *g*. The coerency of the results has been tested using the antropometric tables found in [25,26] and the results are shown in *Tab. 4*.

<b>Mass intervals</b>	$\Delta P_{\max}$ [kPa]	$\Delta P_{\max}$ [%]	$\Delta$ Area [cm <sup>2</sup> ]	$\Delta$ Area [%]	$\Delta$ ots/ns
<b>1-10</b>	-0,69	-17,02	128,13	18,60	-0,15
	0,46	12,02	103,76	10,36	0,12
<b>11-20</b>	-0,38	-11,43	57,63	11,75	-0,11
	0,43	15,31	77,59	15,83	0,12
<b>21-30</b>	-0,15	-4,87	26,71	4,30	-0,10
	0,28	8,93	44,72	11,66	0,10
<b>31-40</b>	-0,29	-10,05	73,54	10,99	-0,09
	0,32	11,43	75,08	14,08	0,12

**Tab. 4** – Mean pressure (in kPa and %), area (cm<sup>2</sup> and %) and over-threshold sensors respect to the active ones differences between the mean of the values in the last and first minute of mattress activity, grouped by mass intervals. In each row are reported the differences between the mean in the last minunte and in the first one of the relative colmn name parameters, while in the row immediately beneath the standard deviations.

As we can see from the comparison of *Tab. 3* and *Tab. 4*, and better from the following figures, this kind of categorization allow us to see even better the efficiency of the mattress depending on the mass that is redistributed.

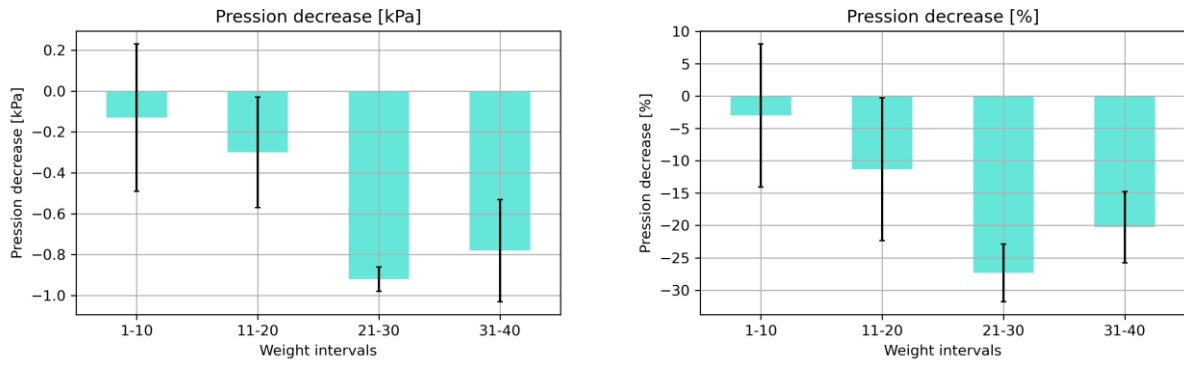


**Fig. 54** – DCPressure decreasing CIP efficiency, expressed in kPa and %, categorized by weight intervals.

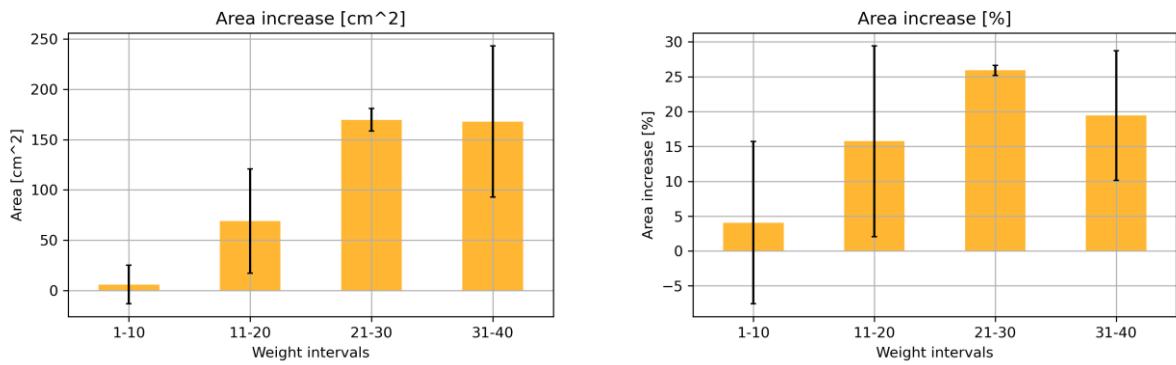


**Fig. 55** – DCPressure increasing area efficiency, expressed in cm<sup>2</sup> and %, categorized by weight intervals.

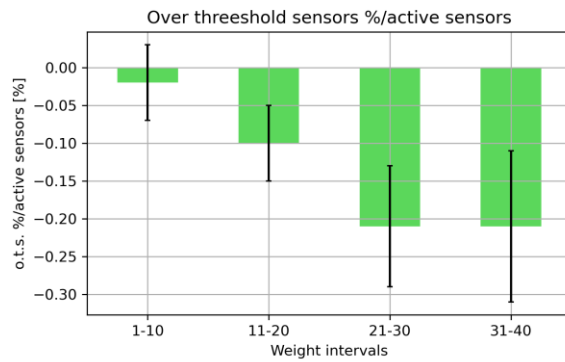


**Fig. 56** - DCPressure decreasing percentage of over-threshold sensors, normalized respect to the total number of active sensors efficiency, expressed in %, categorized by weight intervals.

In the tables and figures above, the characterization of mattress efficiency is categorized by body mass that is on the mattress, but a further consideration must be done on how the mass is redistributed. These graphs and tables are surely more immediate and intuitive for an immediate use of the device, but it should be considered also how the mass is distributed on the cells. Indeed, the antropometric configuration of the human being involves that the heavier areas are also the ones with the higher surface extension. But to underline this aspect, a further division of the data coming from these series of experiments is reported, in which the data are categorized by mass surface density increase, calculated as the mass of the body part under examination [kg] respect to the mean Novel® area involved during the first minute of mattress activity [cm<sup>2</sup>].

M/Area [Kg/cm <sup>2</sup> ]	$\Delta P_{max}$ [kPa]	$\Delta P_{max}$ [%]	$\Delta Area$ [cm <sup>2</sup> ]	$\Delta Area$ [%]	$\Delta ots/ns$
0,02	-0,26	-5,61	16,20	8,55	-0,05
	0,58	15,19	6,95	2,57	0,06
0,03	-0,29	-9,60	60,48	10,38	-0,09
	0,35	12,36	72,70	14,18	0,11
0,04	-0,82	-21,83	180,46	23,60	-0,24
	0,29	6,82	88,06	9,99	0,08
0,05	-0,91	-20,05	142,73	16,87	-0,09
	0,03	0,94	72,97	9,33	0,05

**Tab. 5** – Mattress efficacy in decreasing mean pressure, increasing area and decreasing the number of over-threshold sensors, categorized by body superficial density [kg/cm<sup>2</sup>].

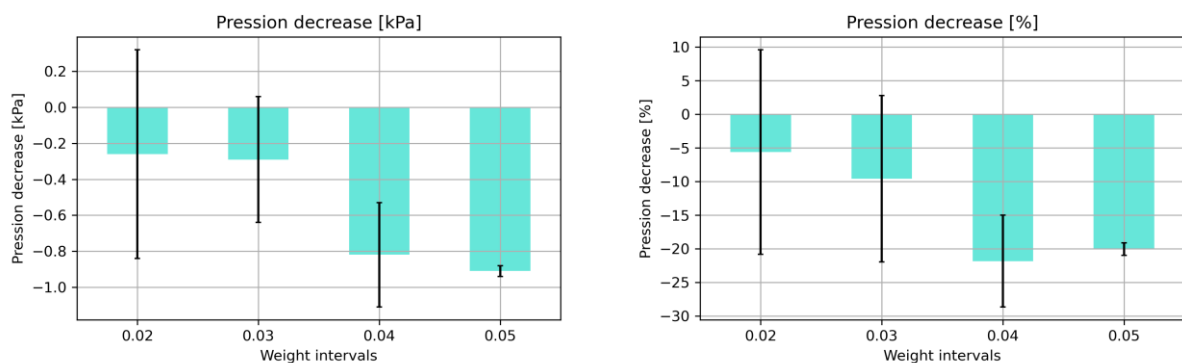


**Fig. 57** - DCPressure decreasing CIP efficiency, expressed in kPa and %, categorized by mass superficial density [kg/cm<sup>2</sup>].

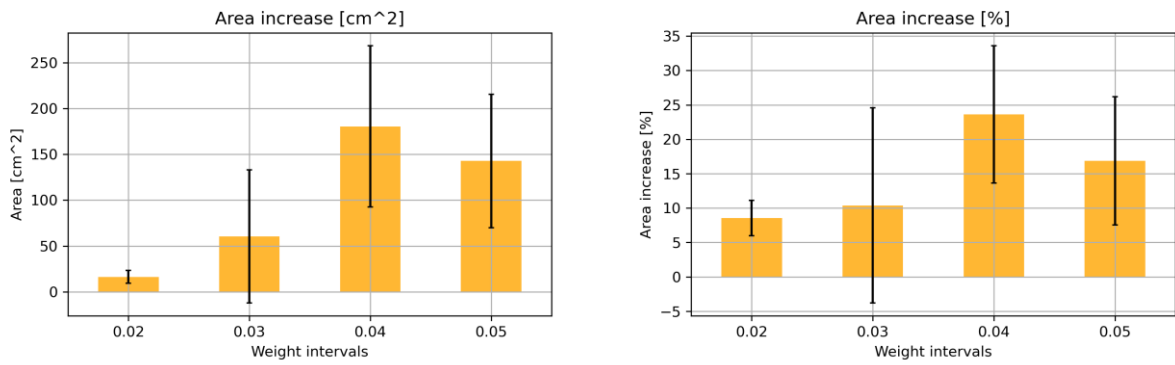


**Fig. 58** - DCPressure increasing contact area efficiency, expressed in cm<sup>2</sup> and %, categorized by mass superficial density [kg/cm<sup>2</sup>].

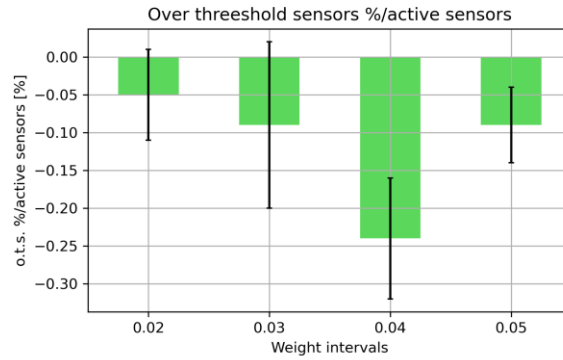


**Fig. 59** – DCPressure efficiency in decreasing over-threshold (30 mmHg) numebr, normalized in respect to the total number of active sensors, expressed in %, categorized by mass superficial density [kg/cm<sup>2</sup>].

### 3.4 Long-term tests

At the end of the 16h test, the weight showed a visible sinking in the center of the area, with a maximum depression of 6 cm respect to the top of the bed, as it is possible to see in *Fig. 62*.



**Fig. 62** – On the left, the weight displacement after 16h of mattress Run mode; on the right the depression left in the area by the weight.

Analyzing the pressure values time evolution of the 16 cells during the test, how it is possible to see in *Fig. 63*, it is possible to appreciate the initial joining of the pressure values in the cells beneath the weight, and the falling of the internal values to levels beneath the initial setpoint values of 0.54 kPa.

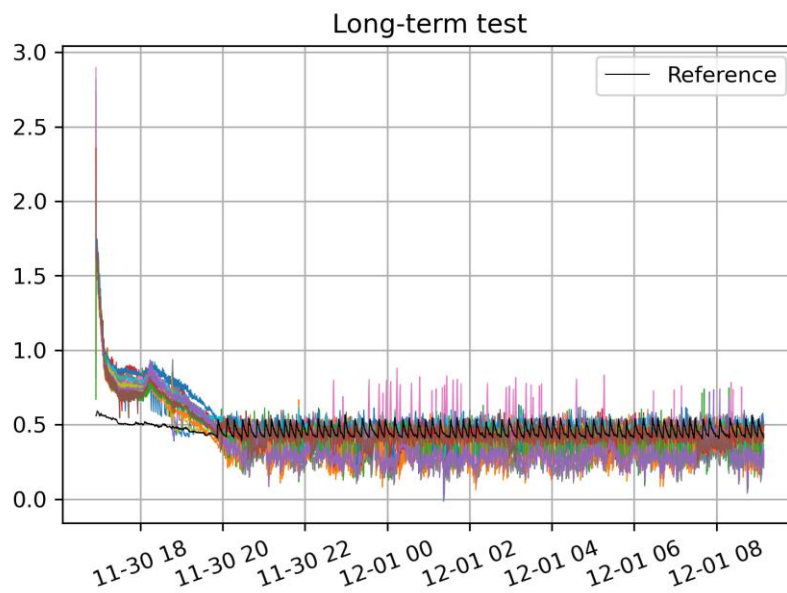


**Fig. 63** – Pressure time evolution of the 16 cells beneath the weight. In black the unloaded cell taken as reference.

At the end of the test, the pressure is manually restored to the initial values, bringing back the load at the top level of the mattress; this last action is performed to verify if the pump is able to inflate a loaded cell and bring it back to the original position.

### **3.5 Calibration Curve**

In this section the calibration of the DCPressure device will be treated; thanks to the measures performed, it is possible to correlate the values of 16 cells for each one of the eight recordings (4 supine and 4 lateral) of the three tested subjects. Dividing the 16 x 16 Novel® matrix sensors in the 16 4 x 4 sensors arrays correspondent to the mattress cells beneath, we have a total of 384 couples of pressure recordings from the Novel® matrix and the DCPressure mattress. These couples have been obtained from the relative mean values of the mean pressure in the first minute of data acquisition of the mattress activity tests.

In this way we have the mean value of pressure recorded by the 4 x 4 Novel® cells array and the correspondent value of mean pressure recorded by the DCPressure mattress, both calculated as mean pressure value in the first minute of the same tests, in which the mattress is inactive. The setpoint values of the mattress cells have been noted and subtracted from the values of pressure recorded by the mattress, to compensate for the different initial pressures. In this way we have now the values of mean pressure recorded by Novel® and the mattress pressure delta, calculated as difference of pressure recorded and the initial setpoints of the cells.

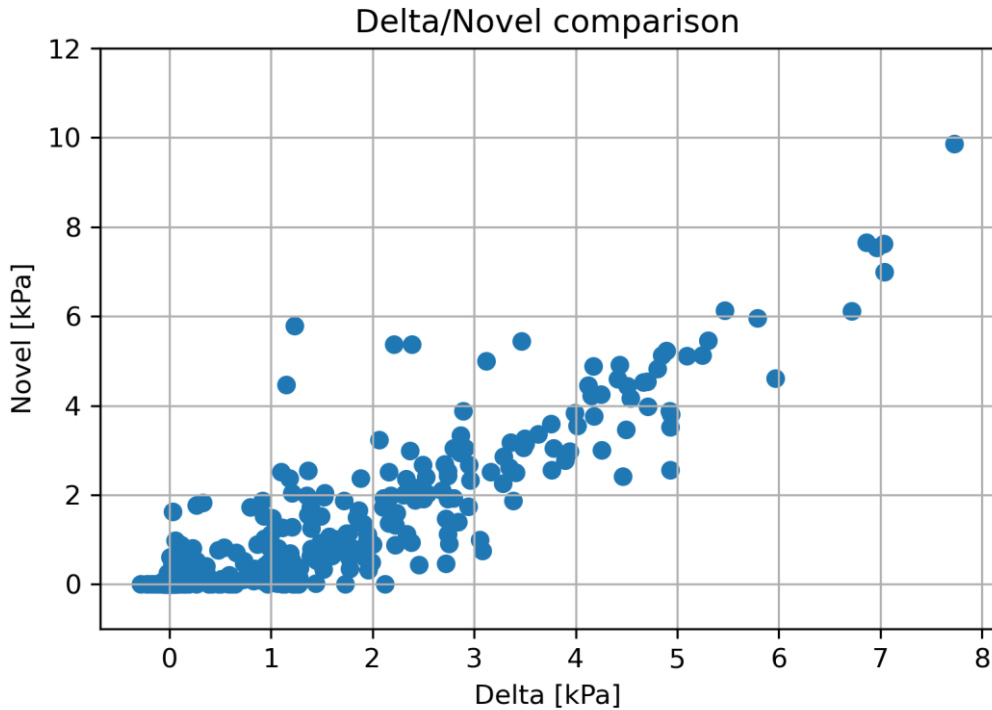


**Fig. 60** – Total number of couples of pression recorded in the 16 cells of the four recordings, in both lying positions, of the three subjects, for a total of 384 points.

From this set, the points where the Novel records a pression equal to zero and the DCPressure doesn't have been discarded, because relative to areas where there is no effective load during the test, but the mattress cell internal pression in that area is bigger than the setpoint, probably due to the compression caused by the adjacent loaded cells. In this way the points number is now 248. A successive data sorting has been performed, not considering the data where the delta is higher than 5 kPa, , bringing the dataset dimension to 236. The points where the pression recorded by Novel® is higher than 4 kPa and the relative DCPressure lower than 4 kPa also have been discarded, to group the points that are better related. From this pruning, starting from the 384 initial points, we now have a set of 157 couples of points to create a regression line that would correlate the measure recoded by the DCPressure mattress and the more precise measure recorded by the Novel® matrix. This set of points is then used to create a regression line, through a least square regressor algorithm: the data composing the set are shuffled randomly and the resulting dataset is then divided into two subset: a training set, used to train the linear regression

algorithm, and a test set to validate it. The training set is composed by the first 80% of the shuffled original dataset, and tested on the remaining 20%.

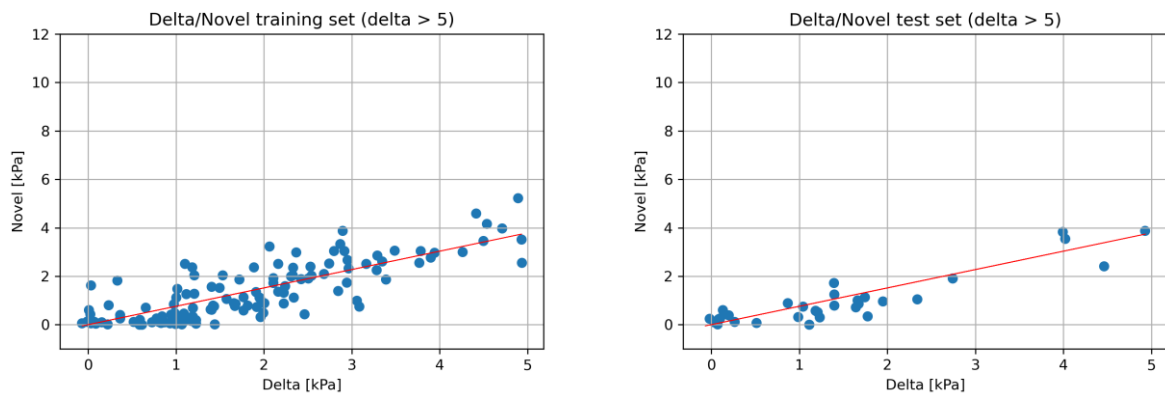


**Fig. 61** – The 80% of the shuffled dataset is used as training set to produce a regression line. This one is then tested on the test set, composed by the last 20% of the shuffled dataset.

To assess the validity of the regression line coefficients, the original dataset was shuffled randomly 10 times in different training sessions, producing in every case a reduction in the RMSE. In the best case, the linear regressor coefficient of 0.76 produced a reduction of the  $RMSE_1 = 0,68$  in the training set with the original data, to a  $RMSE_2 = 0,47$  in the test set with the predicted data, showing a variance of 0,21; the coefficient of determination is 0,80.

## 4. Discussion

The set of tests carried out allow us to assert that, despite a not precise measure of the ICP on the DCPressure cells, the device is quite efficient in decreasing the localized peak pression in all the subjects.

The results of the single cell stress test (*Cap. 3.1*) suggest that the plastic material that encloses the air chambers is suitable for the purpose. The irreversible deformation was reached corresponding to a constantly increasing load maximum of 676 N and an internal recorded pressure of 490 mbar (49 kPa). If the load is exerted for shorter time (681 N for a period of 1s in our case), the internal maximal pression is even higher (500 mbar = 50 kPa), but no deformation has occurred. In no case the deformation caused an explosive behavior of the cells, but only a plastic irreversible deformation of their external shell. These results lead us to validate the material of which the air chambers are made of as suitable for the purpose of the device and not dangerous for the patient or for the mechanical behavior of the system.

For what concerns the ability of a single cell of decreasing a localized pressure peak, the manual deflation of the interested air chamber during the single cell efficacy test (*Cap. 3.2*) highlighted the ability of the design of the system to decrease the maximal pression in the greater tubercle area of subj. 2 lying laterally from an initial pression of 21,70 kPa (162,76 mmHg) to a pressure of 8,56 kPa (64,20 mmHg), with a net decrease of 13,14 kPa (60,25%). It must be said that the pression is still over the threshold, but remembering that the pressure sore risk is proportional to the intensity of ICP by the time, decreasing the contact pressure does not allow to completely avoid the onset of the disease, but could allow to slow down the onset of the symptoms.

Considering instead the total efficiency of the mattress in the reduction of interface contact pressure, increasing the available area, within the DCPressure automatic Run mode, the supine and lateral test (*Cap. 3.3*) highlighted how, with different effectiveness depending on the actuation area, this modality is suitable for reducing the mean and maximal contact interface pression, increasing the area and reducing the number of sensors that record a value higher than the threshold of 30 mmHg. It is important to underline that the three subjects in this test have very different weights, heights and builds, and this is one of the factors that increase the variability of the results in *Tab. 3*, *Tab. 4* and *Tab. 5*. Another factor that helps increasing the variability of the results is the fact that in the classification of the mattress efficiency by body part, the results

coming from the tests carried out with the patient lying supine and lateral have been averaged together when possible. But we should also consider not only the mass that generate the contact interface pressure, but very important is also the interface area and how the mass is in contact with the device. This aspect can be seen in *Tab. 5* and *Fig. 50-52*. Despite these considerations, from the results we can find in *Tab. 3* and *Tab. 4*, we can say that the device efficiency in decreasing the interface contact pressure, increasing the available area and, despite the increased number of active sensors, decreasing the ones recording an interface contact pressure higher than the set threshold of 30 mmHg, increases with the increase of the body mass/surface ratio. For example, the areas of shoulders and hip, that are the heaviest among the one tested, but also the ones that occupy the highest number of cells, are the ones that benefit most from the redistribution of weight and increase in the surrounding area. From the same tables, indeed, we can see that the areas of head and foot are the ones where the ICP decrease is more limited; this happens because, despite the deflation of the cells beneath the area, the interface contact surface remains limited and is not enough to recruit a sufficient number of surrounding cells to redistribute the weight. For the knee, calculated only in the lateral position, we remember you that the interested area concerns also the lower part of the leg and the upper part of the shank, increasing the interface contact area available to redistribute. This aspect can be better seen in *Tab. 5* and the relative figures, where the body mass is in relation with the mean area recruited in the Novel® matrix in the first minute, and the DCPressure efficiency is categorized by the mass that occupies a certain area [kg/cm<sup>2</sup>]. As we can see, the components with a ratio of 0.04 and 0.05 are the ones that benefit more from the pressure redistribution both in terms of pressure decrease and number of over-threshold sensors. This founding agrees with the results of the performances categorized by body mass, which is surely a sorting more effective and quicker to interpret.

Regarding the limitations, how we can see in the calibration chapter (*Cap 3.4*), the measures recorded by the pressure sensors internal to the air chambers is lower than the one recorded by the Novel® matrix. This can be due to the quality of pressure sensor and to the fact that they are not differential, but the pressure value is calculated subtracting the absolute value from the current atmospheric pressure, which is measured with its own imprecision. Despite the imprecision of the internal pressure measurements, this aspect, as we saw from the different 24 test performed, is not affecting the functioning of the device.

In addition, it could be implemented the visualization of mean and maximal pressure values in the active cells that, in addition to the currently implemented colormap, could give to the user a reference value if the pressure is still too high in some areas.

Comparing the overall behavior and performances in decreasing the contact pressure in the automatic run mode and in the manually performed single cell deflating test, in the latter is visible a higher performance in decreasing the ICP. This is due because the human user already knows which are the anatomical points that generate a high contact pressure, in correspondence of the bone prominences, while the current algorithm is more focalized on decreasing the pressure of all the cells considered active. This aspect is less relevant in the areas where the pression is distributed on a wide area, such as the hip or the shoulders, but in the areas where the weight is concentrated on a relative small area, like the malleoli or the elbow, decreasing the pressure in the overall area could not be so effective in decreasing a localized pressure peaks.

This condition could be better implemented inserting in the logic not only the joining of all the cells considered active, but also a comparison of the pressure values of the single cells with the surrounding eight ones. If the values of pressure of the interested cell is higher for more than two system scans compared to the surrounding cells, by a threshold that could be set experimentally, the system could completely deflate the interested cells, while the surrounding ones are deflated less. This for example will guarantee that the areas where the pressure is high and localized in a relative small area, like the greater tubercle or the malleolus when lying on a lateral position, would benefit more from this way of unloading the cells beneath.

Another aspect that could be redesigned is the behavior of the mattress in the long time. During the long-lasting test involving a weight of 30 kg over an area of 16 cells, a lowering of the affected cells to the minimum height levels was found after 16h of automatic Run mode. Watching what happens to the pressure inside the involved air chambers, we can see that the pressure falls under the value of 0.5 kPa after 4 hours. This could be avoided inflating the cells considered active and adjacent ones every 4 hours, bringing them back to the initial memorized pressure level at the beginning of the Run mode, given by the sum of the initial setpoint and the pressure due to the weight of the patient on the cells. This would bring the patient back to the initial condition and initial height level of the cells that have not been deflated; after this process, that it has been verified the current compressor could manage, the Run mode can be restarted.

To conclude, a consideration about the noise generated by the system has to be made: all the three tested subjects considered the ambient too noisy to sleep, and thinking that this system should be implemented in night hospital environments, this aspect must be taken in consideration. An inspection of the device has identified the biggest noise source in the area of the pump/compressor and one of the future steps is strongly suggested to keep in mind the acoustic insulation, but further tests should be performed to clearly individuate with precision the actual noise source component. Some solutions that could be applied are the implementation of an acoustic insulation box around the compressor or the implementation of a dedicated shell to hold the system hardware that takes in consideration this aspect. Another solution could be the evaluation of a low-noise compressor system to replace the one currently in use. The Night Noise guidelines for Europe [27] as well as the communitarian directives (2002/49/CE, 2003/613/CE) delimit a maximum noise in nighttime in a protect area, such as hospital environment of 40 dB. In any case, it should never exceed the 55 dB threshold.

Another aspect that requires a more precise adjustment is the value of pressure delta given to the cells in the massage mode: all the threes subjects, at the end of the eight 10 minutes tests identified as “almost imperceptible” the massage function of the device. This can be improved working on the pressure delta given to the cells during this modality.

In all the cases the mattress current patient detecting logic is able to understand its positioning changes within a minute as time delay.

## 5. Conclusion

The DCPressure prototype, despite some limitations that could be implemented, it is available of understanding the patient position on the bed and decreasing the ICP in automatic modality by 20% on the overall body surface, with a marked efficiency mostly in the hip and thoracic area. The air chamber components never showed an explosive behavior, despite the load exerted, also in the short-time test. The current hardware components are capable to withstand all the system needs of inflation and deflation and can restore to the original state also air chambers completely deflated and subject to load. Nevertheless, a manual control of the cells deflation in a localized area corresponding to a body prominence showed a greater result, and the implementation a logic that pushes to more locally deflate in correspondence of some anatomical areas would greatly benefit the system.

## 6. Bibliography

1. International review. Pressure ulcer prevention: pressure, shear, friction and microclimate in context. A consensus document, London, Wounds International, 2010.
2. Krouskop TA. A synthesis of the factors that contribute to pressure sore formation. *Med Hypothesis* 1983;11(2):255-67.
3. Schubert V, H\_eraud J. The effects of pressure and shear on skin microcirculation in elderly stroke patients lying in supine or semi-recumbent positions. *Age Ageing* 1994;23(5):405e10.
4. Gefen A. How much time does it take to get a pressure ulcer? Integrated evidence from human, animal, and in vitro studies. *Ostomy Wound Manag* 2008;54(10):26e8. 30-35.
5. Kosiak M. Etiology and pathology of ischemic ulcers. *Arch Phys Med Rehabil* 1959;40(2):62e9.
6. Cook AM, Miller Polgar J. *Cook and Hussey's assistive technologies: principles and practice*. third ed. London: Mosby; 2007.
7. Vanderwee K, Grypdonck M, Defloor T. Alternating pressure air mattresses as prevention for pressure ulcers: A literature review. *Int J Nurs Stud*. 2008;45(5):784–801.
8. Wong H, Kaufman J, Baylis B, Conly JM, Hogan DB, Stelfox HT, et al. Efficacy of a pressure-sensing mattress cover system for reducing interface pressure: Study protocol for a randomized controlled trial. *Trials* [Internet]. 2015;16(1):1–11. Available from: <http://dx.doi.org/10.1186/s13063-015-0949-x>.
9. Langemo DK, Melland H, Hanson D, Olson B, Hunter S. The lived experience of having a pressure ulcer: a qualitative analysis. *Adv Skin Wound Care*. 2000 Sep-Oct;13(5):225-35. PMID: 11075022.
10. Lyder CH, Preston J, Grady JN, Scinto J, Allman R, Bergstrom N, Rodeheaver G. Quality of care for hospitalized Medicare patients at risk for pressure ulcers. *Arch Intern Med* 2001; 16: 1549-1554.
11. Maklebust J. Pressure ulcers: the great insult. *NursClin NA* 2005; 40: 365-389.
12. Bain, D. (2011). Laboratory performance of alternating pressure air mattresses. *British*

*Journal of Nursing*, 20(20 SUPPL.), 29–34. <https://doi.org/10.12968/bjon.2011.20.sup12.s29>

13. Manzano, F., Pérez, A. M., Colmenero, M., Aguilar, M. M., Sánchez-Cantalejo, E., Reche, A. M., Talavera, J., López, F., Barco, S. F. Del, & Fernández-Mondejar, E. (2013). Comparison of alternating pressure mattresses and overlays for prevention of pressure ulcers in ventilated intensive care patients: A quasi-experimental study. *Journal of Advanced Nursing*, 69(9), 2099–2106. <https://doi.org/10.1111/jan.12077>.
14. Brown G. Long-term outcomes of full-thickness pressure ulcers: healing and mortality. *Ostomy Wound Manage*, 2003; 49: 42-50
15. Pereira, S., Fonseca, J., Almeida, J., Carvalho, R., Pereira, P., & Simoes, R. (2019). Embedded textile sensing system for pressure mapping and monitoring for the prevention of pressure ulcers. *BIODEVICES 2019 - 12th International Conference on Biomedical Electronics and Devices, Proceedings; Part of 12th International Joint Conference on Biomedical Engineering Systems and Technologies, BIOSTEC 2019, Biostec*, 291–296. <https://doi.org/10.5220/0007690802910296>.
16. Hall CP, Calif MB. Liquid support for human bodies 1971
17. Baharestani MM. The lived experience of wives caring for their frail home-bound elderly husbands with pressure ulcers. *Advances in wound care* 1994; 7: 40-52.
18. LaRossa D, Bucky LP, Witkowski JA, Crissey JT. The decubitus ulcer in clinical practice, Springer 1997; 84.
19. Hall CP, Calif MB. Liquid support for human bodies 1971.
20. May MI. Water bed liner holder, US Patent No 3973282, 1975.
21. Phillips RM. Mattress having an upper internal materialcontaining chamber. 1976.
22. Colwell DJ. Waterbeds, US Patent No 4127908. 1976.
23. McMullan JP, Lindsay RE, Land JE. Water bed with heater, US Patent No 4233492. 1979

24. Chai, C. Y., & Bader, D. L. (2013). The physiological response of skin tissues to alternating support pressures in able-bodied subjects. *Journal of the Mechanical Behavior of Biomedical Materials*, 28, 427–435. <https://doi.org/10.1016/j.jmbbm.2013.05.014>.
25. Charles E. Clauser, *Weight, Volume and Center of Mass of segments of the Human Body*, Aerospace Medical Research Laboratory, Aerospace Medical Division, Air Force Systems Command, 1969.
26. Sofia Scataglini, Gunther Paul, *DHM and Posturography*, 1st Edition, 2019.
27. Rokho Kim, Updating the WHO guidelines on community noise, *The Journal of the Acoustical Society of America*, 131:4, 3294-3294.